Universiteit Utrecht

Deltares
Enabling Delta Life

The behaviour of elemental mercury in porous media

A modelling approach on the multi-phase-flow of elemental mercury

Thomas Sweijen

Supervisors
Prof. Dr. Majid Hassanizadeh
Dr. Annemieke Marsman
Dr. Niels Hartog

Master Thesis
Earth Life and Climate
Utrecht University
4-April-2013

Abstract

Elemental mercury is known for its high density, viscosity and surface tension, making it suitable for a variety of industrial processes, particularly in the past. Nowadays, elemental mercury is a contaminant of concern and occurs in the subsurface at numerous locations. To date however, its behaviour in porous media is not yet fully understood. Therefore, this research focusses on elemental mercury in porous media to establish an understanding of processes characterizing its multi-phase-flow. Such an understanding would enable field simulations of elemental mercury contamination and would enable development of remediation methods. Elemental mercury is a dense-non-aqueous-phase-liquid (DNAPL), given its immiscibility and high density and therefore it is comparable to the better known DNAPL PCE (PerChlorinatedEthylene). In this study, the multi-phase-flow of elemental mercury was modelled for several scenarios by using the numerical simulator STOMP. Modelling results were compared to that of PCE, whilst the use of field observations and literature enabled a close link to reality. In homogeneous saturated porous media, the exceptional high density of elemental mercury governs its flow behaviour, whereas viscosity has a limited influence. The low residual saturation allows elemental mercury to infiltrate substantially deeper than PCE, with the same volume of DNAPL spill. In saturated heterogeneous porous media both elemental mercury and PCE flow via preferential pathways, where the ability of infiltrating less-permeable layers is similar for both DNAPLs. However, elemental mercury migration extends further and is faster than that of PCE, due to the low residual saturation and high density. In the unsaturated zone the behaviour of elemental mercury also deviates from that of PCE, since PCE is wetting to air whereas mercury remains non-wetting. Moreover, when assuming PCE and elemental mercury to be spreading and intermediate wetting, mercury does not infiltrate fine sand whereas PCE does. Finally, this research suggests to validate multi-phase-flow models for the saturated zone and to determine fundamental principles governing three-phase-flow in the unsaturated zone. This could be achieved by experimentally investigating the behaviour of elemental mercury in porous media.

Contents

Chapter 1: Introduction

Elemental mercury is a unique metal: it is liquid at room temperature. It is known for its high density, viscosity, surface tension and electronic conductivity, making it suitable for a variety of industrial applications. It has extensively been used in the past and still is to-date, however elemental mercury usage is being phased-out due to its toxicity to humans (EuroChlor). Consequently, mercury is a pollutant of wide spread concern, in its various forms (e.g. dissolved, organic or elemental form). Its liquid form is considered as a DNAPL or Dense-Non-Aqueous-Phase-Liquid, given its high density and low solubility and hence is comparable to regular organic DNAPLs like PCE (PerChlorinatedEthylene).

The frequent use of mercury results in a variety of historically contaminated sites, in which elemental mercury contamination shows particular features and features similar to regular DNAPLs. For example, in Lavaca Bay in Texas, elemental mercury is found as a DNAPL in the subsurface, resulting from years of waste water disposal into the bay by a chlor-alkali-plant. In Onodaga lake, New York, mercury was found as a DNAPL at depths of 16.8 meters, indicating a severe pollution. In Kodaikanal India, 7 ton of elemental mercury has infiltrated the subsurface. These examples are relics of improper elemental mercury disposal. Elemental mercury in soils might act as a source for soluble, mobile and highly toxic compounds which are hazardous to humans and ecosystems. Therefore these sites are in need of a remediation strategy. Even though, the toxic and mobile forms of mercury have been extensively studied (Gabriel and Williamson, 2004; Wang *et al*., 2012; Horvat *et al*., 2003) a thorough understanding of elemental mercury in soil and groundwater system has not yet been established.

Therefore, this research explores the behaviour of elemental mercury in porous media by using a multi-phase-flow model, to understand the main parameters governing the migration and behaviour of elemental mercury in soil and groundwater systems. In addition, existing knowledge on elemental mercury in porous media is evaluated and used to determine further research questions, for both experimental and modelling research. This research focuses on an artificial and abstract two-phase-flow between water and mercury and gives a preliminary evaluation of three-phase-flow in the vadose zone. This is done by using a numerical multi-phase-flow model STOMP, to evaluate different scenarios, which are compared to other observations (e.g. field-observations). In order to do so, the following questions are addressed:

- Is the current knowledge on DNAPL migration through porous media in a two-phase-flow applicable to elemental mercury? If so, can elemental mercury be modelled and what are the main assumptions to be made?
- What are the controls on the two-phase-flow of mercury with water, how does this compare to PCE, for both transient flow and final distribution?
- Is it possible to model a three-phase-flow system with elemental mercury, if so, what are the major assumptions to be made?
- How do these findings compare with field observations?
- What are the implications of this study for the characterisation and remediation of sites contaminated with elemental mercury?

Chapter 2: Theoretical framework

2.1 Mercury speciation in soil and groundwater systems

This section evaluates mercury speciation in soils and remediation methods. Entrapped elemental mercury can undergo oxidation to form more soluble compounds, which are considered highly toxic to humans (Devasena and Nambi, 2010). The well-studied field of mercury toxicity indicates numerous harmful mercury pollution cases, including: Japan, the Minimata Disease and China (Horvat *et al.*, 2003; Wang *et al.*, 2010). In general, ionic forms might end up in the ecosystem and food-chains, whereas mercury vapour might enhance spreading. The consequence of a mercury spill in the subsurface is highly dependent on the groundwater and soil conditions (Gabriel and Williamson, 2004). In the following section mercury speciation is evaluated by using soil conditions and some accompanying remediation methods are mentioned.

Mercury methylation by bacteria results in highly toxic compounds, which are sensitive to bioaccumulation (Gabriel and Williamson, 2004). This microbial process occurs either in oxic and anoxic environments, producing methyl-mercury and di-methyl-mercury, respectively. Methyl-mercury, a soluble compound, is present in a range of ionic forms, whereas di-methyl-mercury is practically insoluble, but volatile (Gabrial and Williamson, 2004). Methyl-mercury, sensitive to bioaccumulation, ends up in the food-chain and is responsible for the well known Minimate Disease whereas another example is the methyl-mercury concentration in rice, Quinzhen, China (Horvat *et al.*, 2003).

Migration of elemental mercury vapour in the subsurface might enhance mercury spreading in the unsaturated zone. Mercury is not particularly volatile with a vapour pressure of 0.18 Pa, compared to $1.8x10^{-3}$ Pa of PCE (Wang *et al.*,2010; Schwille *et al.*, 1988). Since mercury is toxic at low concentrations its volatility is sufficient for a mercury spill to be a health-risk. From a landfill, elemental mercury may predominately escape directly via upward transport and contribute to the atmospheric mercury content, but lateral transport via the unsaturated zone might occur as well (Walvoord *et al.*, 2010; appendix F). Such a lateral flux results in low mercury concentrations in the surrounding of a landfill and therefore is not considered as an immediate threat. Whereas its vertical compound yields higher concentrations and become a threat to human and ecosystems (Walvoord *et al.*, 2008).

Several remediation strategies for mercury contamination exist, among them is thermal desorption. This method uses the volatility of elemental mercury by heating up soil (Wang *et al.*, 2010). It vaporizes, thus removes, elemental mercury and mercury(II) compounds (e.g. HgO, HgS and $HgCO_3$). For example, 4hr of roasting at 700°C or 20min at 460°C recovers up to 99% of the total mercury content (Massacci *et al.*, 2000; Taube *et al.*, 2008). Therefore this method, though energy expensive, has been used in heavy polluted soils (Wang et al., 2012).

The solubility of elemental mercury is extremely low, hence it is considered an immiscible liquid (i.e. the solubility is 49.6 µg L^{-1} at 20°C; Wang *et al*., 2012). Dissolved mercury is toxic at low concentrations and therefore its low solubility is considered hazardous. Consequently, the maximum allowed concentration in Dutch water is: 0.05 µg L^{-1}(RIVM, 2010). Even more, the speciation of inorganic mercury in soils, depending on redox conditions and pH, varies for different soil conditions. In an oxidizing environment mercury is predominately present in the redox state mercury (II) or Hg^{2+}, whereas in a reducing environment it is Hg^0. At intermediate redox conditions an unstable form, Hg_2^{2+}, is formed and is transformed in either Hg^{2+} or Hg^0 (Schuster, 1991). Under environmental conditions dissolved mercury, Hg^{2+}, predominately forms complexes with OH^- or Cl^- (i.e. $Hg(OH)_2$, $Hg(Cl)_2$). At low or high pH, mercury in complex form is present as $HgCl_2$ or $Hg(OH)_2$, respectively, which is a result of competition between OH^- and Cl^- for adsorption on Hg^{2+} surface (Gabriel and Williamson, 2004; Schuster, 1991).

Adsorption processes, mineral precipitation and complex formation govern mobility of Hg^{2+} and dissolved organic-bound mercury in soils. Adsorption of Hg^{2+} and organometallic mercury in the subsurface delays and retains its spreading and inhibits Hg^{2+} methylation, with the strongest dissolved mercury sorbent being organic matter, followed by metal oxides and clay-minerals (Gabriel and Williamson, 2004). The process of adsorption is governed by the pH and complex formation with Hg^{2+}. At low pH the sorption capacity on surfaces is lower than at high pH, due to the competition of H^+ with Hg^{2+}. Whereas complex formation with Cl^- or OH^- will decrease availability of Hg^{2+}, therefore decreasing the sorption. As a consequence, at low pH and high Cl^- concentration, the adsorption of mercury on mineral surfaces is rather low, whereas at low Cl^- concentration adsorption becomes more favourable (Gabriel and Williamson, 2004; Schuster, 1991).

This process of adsorption is used as a remediation strategy to immobilize Hg^{2+} (Wang *et al*., 2010). For example, pyrite contains sulphur and reacts easily with Hg^{2+}, therefore adding pyrite as nano-particles can retard mercury species via adsorption. This method can be applied both ex-situ and in-situ. Activated carbon and a commercial technique: Silica-Micro-Encapsulation are based on either the principle of adsorbing heavy metals or chemically bind heavy metals, respectively and are both other examples of techniques for Hg^{2+} remediation.

In natural condition Hg^{2+} can precipitate as HgO, cinnabar (HgS), $HgSO_4$ and multiple other solid Hg-compounds (Bernaus *et al*., 2006; Wang *et al*., 2012). In reducing conditions cinnabar predominately precipitates, which is practically insoluble, whereas HgO(s) is a solid more soluble than cinnabar, with a solubility of 0.053 g L^{-1} (at 25°C; Want *et al*., 2012). The solidification process is a remediation method to immobilize Hg^{2+}, which is based on Hg^{2+} precipitation by a chemical binding. For example the reaction of Hg^{2+} with reactive carbon or sulphur, from which the latter one is used in small-scale house-hold mercury spills.

To conclude: the speciation of mercury in groundwater systems is highly dependent on environmental properties, like pH and redox. Remediation methods, based on volatility, adsorption processes or reactions, are available for contaminated soils and groundwater systems.

2.2 Surface properties of mercury

Chemical and physical processes can influence the surface tension of mercury. For this research, it is therefore useful to evaluate different surface properties of mercury, before evaluating its behavior in the subsurface. This is because capillary related effects, for example the concept of wettability is a function of surface tension. Per definition surface tension is the tension of the surface between a liquid and its vapor. The surface tension for elemental mercury is 485 dynes cm^{-1}, however historically measured values can vary between 420 to 500 dynes cm^{-1} (Devasena and Nambi, 2010; Wilkinson, 1972). The interfacial tension is defined as the tension in the surface between two different phases (Wilkinson, 1972; Fetter, 1999). The interfacial tension of elemental mercury and water is 375 dynes cm^{-1} (Wilkinson, 1972). In the case of elemental mercury and air, the interfacial tension is closely related to its surface tension, but can be lowered over long time periods to below 400 dynes cm^{-1} or even to below 300 dynes cm^{-1}, due to adsorption processes (explained further on). To illustrate the influence of several processes on surface tension and hence wettability, this section describes the ranges in which interfacial tensions of mercury can vary. Four aspects are considered: formation of mercury-amalgams, gas adsorption on the mercury surface, water composition influencing interfacial tension and temperature.

During the alkali-process, mercury is used as a cathode in order to facilitate sodium transport via amalgam formation, according to the Castner-Kellner process (Wang *et al*., 2012; EuroChlor). In this manner, elemental mercury contamination in the vicinity of a chlor-alkali plant might be not pure phase mercury but an amalgam with sodium and hence it might exhibit other interfacial- and surface tensions. Implementation of sodium occurs near the interface of elemental mercury and the brine in the Castner-Kellner process; therefore, it will decrease the surface tension of this newly formed amalgam (Wilkinson, 1972). This process might decrease the surface tension of elemental mercury from its original value 485 to 400 dynes cm^{-1} and the decrease is proportional to an increase in sodium concentration. Formation of amalgams can occur with a variety of metals and the surface tension decreases with increasing contamination of mercury (Wilkinson, 1972). This tendency of decreasing surface tension is related to the work function on a molecular level, this however is beyond the scope of this research. So amalgam formation decreases interfacial and surface tensions, which is dependent on the type of amalgam formation.

During a mercury contamination in the environment, mercury is exposed to surface-active-contaminants like gasses and constituents in water. Most atmospheric gasses can adsorb to the surface of mercury, however for inert gasses the change in surface properties can be neglected (Wilkinson, 1972). Even though oxygen is known for oxidizing metals, it does not affect the surface properties of mercury over short time periods. However it might become relevant when some kind of catalyst is present (Wilkinson, 1972). The most particular change in surface tension by interaction with gas originates from reversible water vapor adsorption. It appears that influence of water vapor can be neglected until saturation occurs, then the surface tension drops to the value of the interfacial tension between water and mercury. This is probably due to the presence of a thin water layer around mercury at water saturation. For example: A change of 24 dynes cm^{-1} was recorded for water saturated air, compared to the surface tension of 485 dynes cm^{-1} (Wilkinson, 1972). In summary, the interfacial and surface tensions decreases over time when surface-active-contaminants are

present, for different rates and lists of surface-active-compounds, the reader is referred to Wilkinson, 1987 and references therein.

The water composition seems to be important for the interfacial tension between water and elemental mercury. Different studies have been conducted on the influences of oxygen and carbon dioxide in water on the surface tension of mercury. It appears that in a natural situation, with water including carbon dioxide and oxygen, the interfacial tension is about 375-380 dynes cm^{-1} (Wilkinson, 1972). However, particular features occur on the wettability of water when changing the pH, during dynamic or kinetic wettability. When adding a droplet of acid water onto a mercury surface, water will spread, but when adding a base solution, it will not spread on the surface of mercury. Therefore, it seems that wetting of a mercury surface by water is pH dependent, however no pH thresholds for this phenomenon are given. When the pH of groundwater ranges from 6 to 9, this pH dependency and water composition might become important for the movement of mercury in soils.

Finally, surface tension is proportional to a change in temperature. This relationship is well documented by several articles (Wilkinson, 1972). The surface tension of elemental mercury will decrease linearly with increasing temperature, for experimental data this is: -0.224±0.032 dynes cm^{-1} $°C^{-1}$. Elemental mercury in the environment will be subjected to a temperature ranging between 10°C and 25°C, therefore the surface and interfacial tensions, which are measured at 25°C, will be higher at 10°C: +2.24 dynes cm^{-1}. This however is a minor change, when comparing it to other surface tension differences and therefore temperature dependency is neglected in this research.

2.3 Principles of mercury in multi-phase-flow

In hydrogeology, the wettability of a fluid is important in multi-phase flow. It affects the mobility of a fluid, the relative permeability and thus the residual saturation. The wettability of a substance is the tendency of a fluid to wet a surface above another substance (Fetter, 1999). This concept becomes important during multi-phase flow modelling, since a non-wetting fluid is entrapped by a wetting fluid and governs the relative permeability (Mayer and Hassanizadeh, 2005). In the case of a porous media, the wettability of an immiscible substance is measured with respect to another substance and a solid. Between two phases an interfacial tension is present, which resembles chemical and physical interactions and is defined as the amount of work that is required to separate two phases from each other per surface area. When making an interfacial tension balance in a given system, a contact angle is needed to satisfy equilibrium (fig. 1). This is described by a line tension balance with σ being the interfacial tension between two substances, described in the subscript and θ the contact angle:

$$\sigma_{ma} \cos \theta_{ma} = \sigma_{sa} - \sigma_{ms}$$

$$cos\ \theta = \frac{\sigma_{sa} - \sigma_{ms}}{\sigma_{ma}}$$

where *ma* denotes mercury-air, *sa* solid-air and *ms* mercury-solid. The wettability of a fluid is defined by the contact angle with the solid, measured through its fluid body with respect

to another fluid, by convention 0°<θ<180°. When 0°<θ<90°, then the substance is thought to wet the surface of a solid, when 90°<θ<180°, the substance is non-wetting. Two exceptional cases are that θ is 0° or θ is 180°, the substance is completely wetting or non-wetting, respectively (Fetter, 1999). This method gives the wettability of a fluid in a two-phase system, compared to a certain solid. Experimental data for the contact angle with a solid in respect to another substance can be obtained by doing several tests, for example a capillary-test, in which a small tube made of a certain solid is put into a container with a certain substance. As a result the substance will go into the tube and a meniscus will arise and gives the contact angle (with air being the other substance).

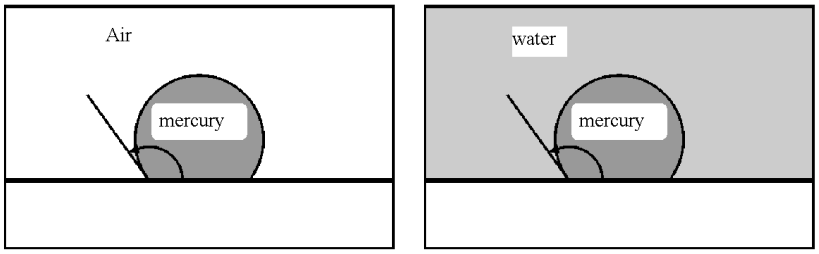

Fig. 1: Wettability phenomenon for elemental mercury on quartz in air or water, respectively.

Typically, it is thought that porous media are water-wet; therefore both air and NAPL are the non-wetting phases in two-phase-flow. For regular NAPLs, like PCE and TCE, it is assumed to be wetting to air and non-wetting to water, in respect to water-wet solids, i.e. intermediate wetting. Elemental mercury, however, is non-wetting in a two-phase-flow with air, this phenomena is used in mercury-intrusion-porosimetry (MIP), with an average contact angle of 130° (appendix D; Rigby and Edler, 2002; Romero and Simms, 2008). In addition, water is wetting compared to air and therefore water is also wetting compared to mercury in a two-phase-flow, with an estimated contact angle between water-mercury being θ_{mw} 150.3° (appendix A). This is confirmed by the presence of an entry pressure for elemental mercury flowing into a saturated porous media (Devasena and Nambi, 2010). So, air preferential wets the surface rather than elemental mercury and therefore deviates from regular NAPLs, such as PCE (Cohen and Mercer, 1990).

In a three-phase-flow system with high NAPL saturations (i.e. water, air and NAPL) it is generally assumed that the porous media is water wet and that NAPL will form a thin layer between the water-air interface upon infiltration (Hofstee *et al*., 1998). At lower saturations, on the other hand, NAPLs might form a droplet on the water-air interface rather than infinitely spreading, this is dependent on the interfacial tension balance and determines whether a NAPL is spreading or non-spreading (Fig. 2). In order to accomplish a line tension balance, the following balance should be true:

$$\sigma_{aw} = \sigma_{ao} cos\theta_{ao} + \sigma_{wo} cos\theta_{wo}$$

where *aw* denotes air-water, *ao* air-NAPL, *wo* water-NAPL. The contact angles are supposed to be 0, in order to maintain a continuous flow (Hofstee *et al*., 1998). For spreading NAPL's this assumption remains valid when reaching residual saturations (i.e. pressure equilibrium). For non-spreading NAPL's this assumption will not be true and contact angles will arise, during formation of discontinuous lenses (Hofstee *et al*., 1998).

The spreading-ness of a NAPL is the tendency of a NAPL to spread on the water-air surface on pore-scale and is determined by using the spreading-coefficient (∑).

$$\Sigma = \sigma_{aw} - (\sigma_{oa} + \sigma_{ow})$$

When ∑<0 then the liquid is a non-spreading NAPL and when ∑>0 then the liquid is a spreading NAPL. The spreading-coefficient is based upon the balance between interfacial tensions and indicates the difference of forces acting on the triple point. For example, PCE is a non-spreading NAPL and so is mercury, assuming a water-wet porous media (PCE; according to Hofstee *et al*., 1998; mercury ∑=788 dynes cm^{-1} by using typical interfacial tensions; table 2.). However, for applying the spreading-coefficient in a three-phase-flow, water is assumed to be wetting and air to be non-wetting, which is likely but has not been experimentally determined for mercury.

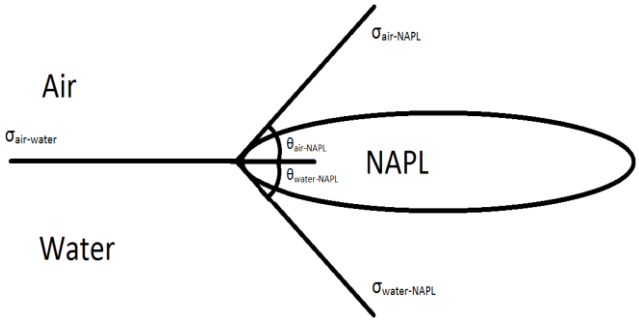

Fig. 2: Line tension balance in an artificial three-phase-system on micro scale with NAPL as intermediate wetting phase in a water-wet porous media. NAPL can be either spreading or non-spreading, depending on the interfacial tension acting.

2.4 Infiltration of elemental mercury in groundwater and soil systems

One of the unknown phenomena of elemental mercury in the subsurface is its entry-pressure, hence the possibility of mercury to infiltrate soil and groundwater systems. It is thought that the water saturation controls the entry-pressure of mercury. Eichholz *et al*., 1988 showed that elemental mercury would infiltrate a soil column under a 1mm mercury head, but did not exceed a depth of 3 á 4 cm. Consequently, it was concluded that in this hypothetical landfill, mercury would not extensively infiltrate the soil column under commonly occurring elemental mercury head (i.e. 1mm). However, elemental mercury was found as a DNAPL in Onodaga lake, New York and in Lavaca Bay, Texas (Deen *et al*., 2011; ITRC, 2012; Scanlon *et al*., 2005). So, elemental mercury does infiltrate soil and groundwater systems, but apparently it is dependent on the soil type and other conditions.

Elemental mercury has an entry-pressure in both saturated and dry soil, whereas PCE has solely an entry-pressure in saturated soil. Per definition a non-wetting phase has an entry-pressure, whereas a wetting phase has no entry pressure, according to Youngs-Laplace equation (i.e. $\theta < 90^{\circ}$ results in a $Pe < 0$ Pa):

$$P_e = -\frac{2\sigma \cos\theta}{r}$$

where *r* is the pore throat radii and *Pe* the according entry-pressure. Where PCE would infiltrate a dry soil under 1mm head, elemental mercury would not infiltrate. This because the entry-pressure of elemental mercury is higher than 1mm for common soils, hence explaining the lack of infiltration found in the research by Eichholz *et al*., 1988 (as explained in the following paragraph). In summary, elemental mercury has an entry pressure for both saturated and dry soil whereas PCE has only an entry-pressure for saturated soil.

To quantify entry-pressures for NAPLs in different porous media, Leverett scaling is often used. It is based on correcting the entry-pressure for the difference in fluid-fluid interactions between two fluids, in this manner water-air entry-pressures can be transferred to NAPL-water entry-pressures. This correction factor is based on Leverett's equation for entry-pressure, similar to Young's Laplace equation:

$$P_e = \frac{2\sigma}{r'}$$

where *r'* is the representative pore radii. The method of Leverett-scaling is defined as follows, assuming the pore-radii to be constant:

$$\frac{P_1}{P_2} = \frac{\sigma_1}{\sigma_2}$$

In this manner, known entry-pressure for air in water-air systems can be extrapolated to mercury-water and mercury-air systems.

Devasena and Nambi, 2010, have conducted short column experiments on elemental mercury in saturated coarse and medium sand. It was suggested that elemental mercury was Leverett scalable in saturated medium and coarse sand, with entry-pressures of 2.15 and 1.37 cm of mercury head, respectively. Or 2.77 or 1.77cm for dry soil by Leverett-scaling, hence explaining the lack of infiltration found in the article of Eichholtz *et al.*, 1988. Figure 3 shows the aforementioned entry-pressures for saturated porous media and Leverett-scaled entry-pressures for typical soils as a function of grain diameter, to illustrate the quality of the prediction by Leverett-scaling (table 2). It is assumed that grain size is linear proportional to the pore and pore-throat radii (Fetter, 1999). The fitting of experimental data with predicted data appears to be reasonable, where entry-pressures for elemental mercury are slightly lower for experimental data than the scaled data. Therefore, scaling of the entry-pressure for elemental mercury is assumed to apply, even though experiment proof suggests a small deviation.

Another feature of elemental mercury is its ratio between density and interfacial tension compared to that of PCE. This ratio is used for determining the entry-head of elemental mercury from water-air entry-pressures, for elemental mercury:

$$h_{Hg}^{mw} = h_{H2O}^{wa} * \frac{\rho_w}{\sigma_w} * \frac{\sigma_{Hg}}{\rho_{Hg}}$$

where h_{Hg}^{mw} is the entry-head of elemental mercury in an elemental mercury-water system [cm of mercury], h_{H2O}^{wa} is the entry-head of air [cm of water]. The ratio between interfacial tension and density of elemental mercury is similar to that of PCE:

$$\frac{\sigma_{Hg}}{\rho_{Hg}} = \frac{375}{13.500} = 0.028 \left[\frac{dynes\ cm^{-1}}{kg\ m^{-3}}\right] \qquad \frac{\sigma_{PCE}}{\rho_{PCE}} = \frac{44.4}{1.650} = 0.027 \left[\frac{dynes\ cm^{-1}}{kg\ m^{-3}}\right]$$

Consequently, the entry-head for both elemental mercury and PCE yields the same height. This is reflected in the bond number for elemental mercury and PCE, which is in the same order of magnitude. The bond number illustrates the importance of gravitational forces over capillary forces, whereas the capillary number illustrates the importance of viscous forces over capillary forces:

$$N_B = \frac{(\rho_{nw} - \rho_w) g r^2}{\sigma}$$

$$N_C = \frac{\mu_w U_w}{\sigma}$$

where μ_w is the viscosity of the wetting fluid and U_w is the flow velocity of the wetting fluid. The bond number and capillary number for PCE and elemental mercury are given in table 1, which indicates the bond number for PCE and elemental mercury to be in the same order of magnitude. So, the ratio of density and interfacial tension for both PCE and elemental mercury are rather similar, which is reflected in known bond numbers for both DNAPLs.

In summary, the entry-pressure for elemental mercury seems to be predicted by Leverett scaling. The ratio of density and interfacial tension are for both DNAPLs similar, hence the entry-head required for infiltrating a soil is approximately equal for both DNAPLs.

	Nb		***Nc***	
	Coarse sand	*Medium sand*	*Coarse sand*	*Medium sand*
PCE	3.2x10-5	0.5x10-5	1.71x10-8	0.36x10-8
Elemental mercury	8.2x10-5	1.3x10^-5	4.8x10-9	1.2x10-9

Table 1: Bond- and capillary numbers for PCE and elemental mercury for coarse- and medium sand (Devasena and Nambi, 2010).

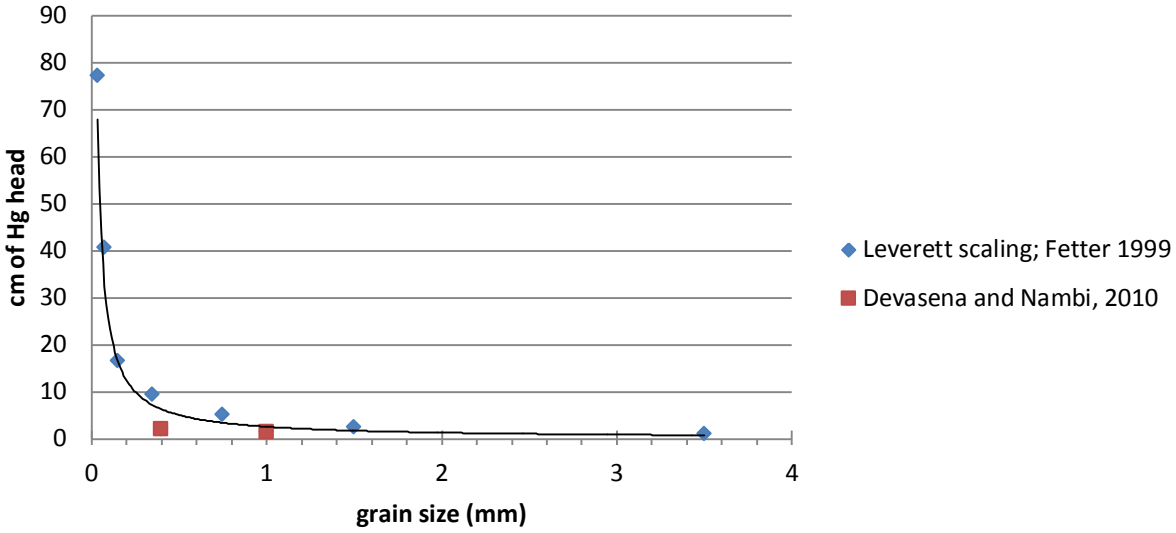

Fig. 3: Entry-head of elemental mercury as function of grain size. Solid line is the fitting for all data, which is given by the formula $h_e = 2.554r^{-0.979}$ *with a R²=0.886. Hence, entry-head is invers proportional to pore radii.*

Material	*Grain size (mm)*	*Repr. Grain size (mm)*	*Capillary Rise (cm)*	*Entry-pressure elemental mercury (cm of Hg)*
Fine gravel	2 to 5	3.5	2.5	1.25
Vercy coarse sand	1 to 2	1.5	6.5	3.24
Coarse sand	0.5 to 1	0.75	13.5	6.74
Medium sand	0.2 to 0.5	0.35	24.6	12.27
Fine sand	0.1 to 0.2	0.15	42.8	21.36
Silt	0.05 to 0.1	0.075	105.5	52.64
Fine silt	0.02 to 0.05	0.035	200	99.79

Table 2: Capillary rise of water for several typical porous media, with the Leverett-scaled entry-pressures for elemental mercury.

2.5 Multi-phase-flow model

In this research a multi-phase-flow model is used, enabling modelling of elemental mercury in the subsurface. Multi-phase-flow is flow of multiple immiscible fluids through porous media. The governing equations of multi-phase-flow models are described by Darcy's law (Fetter, 1999; Mayer and Hassanizadeh, 2005). It assumes a continuous flow and a domain larger than a so called REV (Representative Elementary Volume), which implies parameters to be an average over a certain domain rather than a local value. Therefore, it is suitable for simulating large-scale problems and not for micro-scale problems. Darcy's law for each separate phase in a multi-phase-flow is given by:

$$\bar{q}_\beta = -\frac{k_{r\beta}k}{\mu_\beta}\left(\nabla p_\beta + \rho_\beta g \nabla z\right)$$

where $\bar{q}_\beta$ is the Darcy velocity for phase β, $k_{r\beta}$ the relative permeability for β, k the intrinsic permeability, μ_β the viscosity of β, ∇p_β the pressure gradient for phase β, ρ_β the density of phase ρ_β, g the gravitational acceleration and z the upward unit vector. This is combined with a mass balance for each separate phase:

$$\phi\frac{\partial \rho_\beta S_\beta}{\partial t} = -\nabla \cdot \left(\rho_\beta \bar{q}_\beta\right)$$

where S_β is the saturation of phase β and ϕ the porosity. Per definition saturation is the fraction of void space within a porous media which a phase occupies.

Several constitutive equations are needed for connecting the mass balance and Darcy's law for each phase, to obtain an overall governing set of equations. First, a volume balance for multiple phases is given, which states that water, NAPL and air occupies the total void space:

$$S_w + S_o + S_a = 1$$

where S is the saturation and w denotes water, o denotes NAPL and a denotes air. Finally, the concept of capillary pressure connects these equations to allow numerical solving. The concepts on capillary pressure and relative permeability are discussed in the next section.

2.5.1 Capillary pressures and saturation definitions

In pore and pore throats, a curved interface between two immiscible fluids is present, due to a difference in interfacial tension (i.e. the concept of wettability). Consequently, a capillary pressure arises to account for the fluid-fluid interactions and is described by the difference in pressure of the wetting fluid and the pressure of the non-wetting fluid:

$$P_c = P_w - P_{nw}$$

where P is the pressure, c denotes capillary pressure, w the wetting fluid and nw the non-wetting fluid. It is assumed that a two-phase-flow has one interface between two fluids and

a three-phase-flow has two interfaces: water-NAPL and air-NAPL (Lenhard, 1994). Hence, the capillary pressure is given by:

$$P_{cow}(S_w) = P_o - P_w$$
$$P_{cao}(S_t) = P_a - P_o$$

where *cow* denotes capillary pressure between NAPL and water and *cao* denotes capillary pressure between air and NAPL. During a multi-phase-flow with a water-wet porous media and NAPL as intermediate wetting phase, it is assumed that NAPL will spread on the water-air interface (Hofstee *et al.*, 1998). The capillary-saturation function, described in the next section, relates the capillary pressure of water-NAPL to the water saturation and the capillary pressure of NAPL-air to the total liquid saturation. Total liquid saturation is the sum of all liquids and entrapped air:

$$S_t = S_w + S_o + S_{at}$$

where *t* denotes total and *at* denotes trapped air by either NAPL or water. Water saturation is given by:

$$S_w = S_w + S_{ot} + S_{atw}$$

where *ot* denotes NAPL trapped by water and *atw* denotes air trapped by water. These definitions enable efficient solving of the model, but assume that water is wetting and can entrap NAPL and air, NAPL is intermediate wetting and can entrap air and air is non-wetting and can entrap no fluid (Parker and Lenhard, 1987).

2.5.2 Pc(S) functions and relative permeability

To quantitatively describe capillary-pressure or Pc(S) curves the van Genuchten or Brooks-Corey function can be used (van Genuchten, 1980; Mayer and Hassizadeh, 2005). These functions are based on effective saturations [0,1] to include hysteresis. Hysteresis is a result of difference in contact angle during drainage, the process of infiltrating non-wetting phase, and imbibition, the process of infiltrating the wetting phase. As a consequence residual non-wetting phase and irreducible water content arise during flow processes. To link effective saturation to saturation, it is normalized to the irreducible water saturation. In this manner the shape of Pc(S) curves can be transferred to any range of saturations between irreducible- and residual saturations. This scaling sets the irreducible water saturation to $\bar{S}$=0, such that the y-axis becomes the asymptote of this curve. So S_{irw} is used for normalizing absolute saturations (S) to effective saturations ($\bar{S}$) such that the effective water and NAPL saturation are given by:

$$\bar{S}_w = \frac{S_w - S_{irw}}{1 - S_{irw}}$$

$$\bar{S}_o = \frac{S_o}{1 - S_{irw}}$$

where $\bar{S}$ denotes effective saturation. So the Pc(S) curves are described by Brooks-Corey or van Genuchten functions, which are dependent on the soil type, even thought Pc(S) is soil and fluid property dependent. Therefore a scaling method is applied to account for fluid-fluid interaction, the so called Leverett-scaling as described in section 2.4 (Parker and Lenhard, 1987b; Lenhard, 1994; Leverett, 1941). First the retention curves are described and then the scaling method. Pc(S) curves are given by either Brooks-Corey or van Genuchten and are thought to be soil specific, therefore the van Genuchten parameters n, α and Brooks-Corey parameters h_d and λ and finally S_{irw} are also soil properties. The Brooks-Corey retention curve is given by:

$$\bar{S} = \left(\frac{P_d}{P_c}\right)^{\lambda} \qquad \text{for} \quad P_c > P_d$$
$$\bar{S} = 1 \qquad \text{for } P_c < P_d$$

where, λ describes the pore size distribution and P_d describes the entry pressure and P_c is the capillary pressure. This function shows a discontinuity in the retention curve at fully water saturation (S_e=1), since an entry pressure is needed to enter porous media. The van Genuchten function for retention curves does not show this discontinuity, but appears to have a slightly better correlation with experimental data, even though both approximations are relatively good (Lenhard and Parker, 1987a; Mayer and Hassanizadeh, 2005). The van Genuchten function is given by:

$$\bar{S} = (1 + (\alpha h_c)^n)^{-(m)}$$

with

$$m = 1 - \frac{1}{n}$$

where the parameter α and n describes the soil properties and h_c is the capillary head (Van Genuchten, 1980). In general, Pc(S) curves are determined by doing short column experiments (Lenhard and Parker, 1987b; Devasena and Nambi, 2010). In order to limit the amount of experiments, a scaling method is used to scale water-air Pc(S) curves to Pc(S) curves for water-NAPL, even more this scaling method is used to determine Pc(S) curves for two capillary pressures used in three-phase-flow: P_{cow} and P_{cao} (Lenhard and Parker, 1987; Lenhard, 1994). It is based on the van Genuchten or Brooks-Corey function for soil retention curves, on which a scaling factor is applied (Parker and Lenhard, 1987; Lenhard and Parker, 1987a). The scaling factor corrects the capillary pressure for the difference in interfacial tensions between water-air and NAPL-water or NAPL-air (Lenhard and Parker, 1987a). As mentioned before the total liquid saturation is dependent on P_{cao} and the water saturation is dependent on P_{cow}, therefore the constitutive scaling is:

$$S_w(\beta_{ow} h_{ow}) = S(h)$$
$$S_t(\beta_{ao} h_{ao}) = S(h)$$

where S(h) represents the soil Pc(S) relation, for water-air, h is the pressure head between two substances and β is the corresponding scaling factor. The pressure head is defines as:

$$h_{ij} = \frac{(P_i - P_j)}{g\rho_w}$$

where *i* and *j* denotes different phases. The scaling factor used is the ratio of the interfacial tension between the two phases (σ_{ij}) and a reference interfacial tension (σ^*):

$$\beta_{ij} = \frac{\sigma^*}{\sigma_{ij}}$$

The reference interfacial tension for regular NAPLs can be either the interfacial tension between water and air: 72 dynes cm^{-1} or the sum of the interfacial tension between NAPL-water and NAPL-air (Lenhard, 1994; Lenhard and Parker, 1987a). Where the latter one is proven to be valid and does not yield a discontinuity in pressure-saturation curves for a multi-phase-flow system, whereas assuming the reference interfacial tension to be 72 dynes cm^{-1} does include a discontinuity. (Lenhard,1994).

Finally, the concept of relative permeability determines the permeability of each separate phase as function of its saturation. Fluids in porous media compete for pore space, the higher its saturation, the higher its permeability (Fetter, 1999). The relative permeability [0,1] states which fraction of the total permeability belongs to one single phase:

$$k_\beta = k \times k(S)_{r\beta}$$

where k_β is the permeability of phase β and $k(S)_{r\beta}$ is the relative permeability as function of saturations. It is determined by using either van Genuchten or Brooks-corey function and Mualems- or Burdines model. In this study van Genuchten- Mualem's model is used and is given by (Lenhard and Parker, 1987a):

$$k_{rw} = \bar{S}_w^{1/2}\left[1 - (1 - \bar{S}_w^{1/m})^m\right]^2$$

$$k_{ra} = (1 - \bar{S}_t)^{1/2}\left(1 - \bar{S}_t^{\,1/m}\right)^{2m}$$

$$k_{ro} = (\bar{S}_t - \bar{S}_w)^{1/2}\left[\left(1 - \bar{S}_w^{\,1/m}\right)^m - \left(1 - \bar{S}_t^{\,1/m}\right)^m\right]^2$$

In summary, this closed set of equation enables modelling of multi-phase-flow. Darcy's law, the mass balance and a constitutive set of equations are the basis for numerical solvers, where Pc(S) curves and the according relative permeability can be chosen from van Genuchten or Brooks-Corey and Mualem's or Burdine's model. The constitutive relations used in this model imply a continuous spreading liquid with a finite relative permeability (Oostrom *et al*., 2003).

Chapter 3: Methods

3.1 Numerical model

To study multi-phase-flow processes involving mercury in soils, STOMP or Subsurface Transport Over Multiple Phases was used (White and Oostrom, 2000). It is based upon the computational language FORTRAN 77, and it solves the aforementioned set of differential equations numerically, by using Newtons-Ralphs iteration method. It is a three dimensional computational program, which is capable of modelling multi-phase-flow, ground-water-flow, solute transport and multiple other processes. During this research, the STOMP module water-oil was used. It assumes a three-phase-flow between water and NAPL, with a passive air phase. This model has been used frequently in studies, for validation purpose (Hofstee *et a.l*, 1998; White and Lenhard, 1993). In the following section the model domain, initial and boundary conditions and finally the model scenarios are discussed.

3.1.1 Model domain

For this research a DNAPL infiltration was modeled in both homogeneous and heterogeneous soils, for both fully saturated and partially saturated aquifers. A semi-3D-model domain was designed to model the saturated zone, such that boundaries would not interfere with PCE or elemental mercury movement. The model was sized 25m by 1 m by 50m with a grid of 25x1x50 cells (fig. 4A). Where no convergence was achieved the grid size was refined (e.g. lithology interfaces, boundary condition).

A smaller model domain was designed to illustrate heterogeneities in the vadose zone, as was done by Hofstee *et al*., 1998. It was sized 170cm by 5cm by 100cm with a grid of 30 by 1 by 33 cells (fig. 4B). In summary, two model domains were used during this research, for the saturated zone, partially saturated zone and the unsaturated zone.

A B

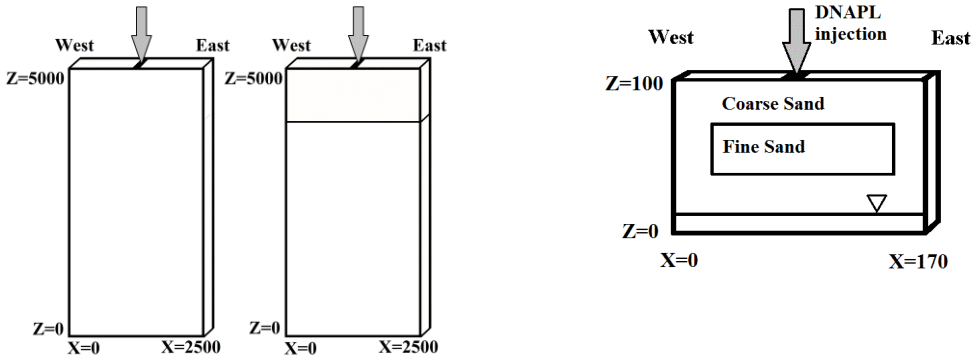

Fig. 4a): The 2D domain used in this research, was designed to investigate two-phase-flow processes between water and mercury or PCE. The size is 25 by 1 by 50 meters. A DNAPL spill was simulated by a pulse injection into the porous media on top of the model, indicated with an arrow. Left) a fully saturated domain, right) a partial saturated zone with the water table at Z=4000cm. 3b) The 2D domain used in this research, was designed to investigate the three-phase-flow in the vadose zone. The size is 170 by 5 by 100cm. Porous media made of coarse sand with a fine sand heterogeneity. A DNAPL spill is simulated by a pulse injection into the porous media on top of the model, indicated with an arrow.

3.1.2 Initial and boundary conditions

Initial and boundary conditions were chosen to represent a DNAPL pulse injection in a saturated or unsaturated zone. Initial conditions resembled a hydrostatic groundwater distribution, by applying a constant aqueous pressure at Z=0 and implying a hydraulic gradient (table 3). Boundary conditions were chosen to maintain the initial conditions by implying a hydraulic gradient at the west and east side of the model and a constant pressure at the model bottom. The hydraulic gradient is defined as:

$$\frac{dP_h}{dZ} = -(\rho_w g)$$

where, P_h is the hydraulic pressure [Pa], Z is the depth [m], ρ_w is the density of water [kg m^{-3}] and g is the gravitational acceleration [m s^{-2}]. A fully saturated zone was achieved by a constant aqueous pressure at Z=0 which is defined as:

$$P_{h,Z=0} = P_a + 50 \times \left|\frac{dP_h}{dZ}\right|$$

where P_a denotes the atmospheric pressure. In the same manner, pressure at Z=0 for the unsaturated zone was determined. This data was implemented in the model to obtain a hydrostatic groundwater distribution.

Boundary conditions resemble a DNAPL spill, by using a pulse injection. A Dirichlet boundary condition, equal to 90cm head of mercury over 1m² surface, was chosen to simulate a contamination, resembling one leaking Castner-Kellner cell with brine on top of the mercury. The volume of elemental mercury contamination was set on 1.5m³ (equivalent to 20.250 kg of mercury), since 65 tons per year was unaccounted for in the United States in the year 2000 (EPA, 2003). This is an average of 7 tons per chlor-alkali-plant per year, therefore 1.5m³ or 20.250 kg is assumed to be an average of unaccounted mercury volume, for over three years of contamination. By using a constant volume of NAPL contamination for both PCE and elemental mercury, the density was considered a fluid property, which is an important parameter for multi-phase-flow. To achieve the correct volume of DNAPL a certain amount of time was required for infiltration, which differed for each fluid and scenario. Nevertheless all injections were considered pulse injections.

Physical property		*Unit*	
Gravitational acceleration	9,81	M s^{-2}	
Atmospheric pressure	101325	Pa	*Default* value STOMP-WO
Hydraulic gradient	-9789,284	Pa m^{-1}	
Aqueous pressure at Z=0	590789,2	Pa	Water table at Z=5000cm
Aqueous pressure at Z=0	492896.0	Pa	Water table at Z=4000cm
Aqueous pressure at Z=0	102303.9	Pa	Water table at Z=10cm
NAPL pressure (Z=50m)	216102	Pa	

Table 3: Physical properties for hydrostatic groundwater distribution and NAPL pressure at the boundary condition.

3.1.3 Model scenarios

In this research the behaviour of elemental mercury was illustrated in several model scenarios, each of them gave insight by doing a certain analyses, described in this section.

Scenario A: Saturated homogeneous medium sand. This scenario was used for multiple purposes. To illustrate the fundamental differences between PCE and elemental mercury after a DNAPL spill of 1.5m³. Also, sensitivity analyses were done on mercury to determine the influence of viscosity and density.

Scenario B: Mercury wet-porous media in a homogeneous medium sand aquifer. This scenario was used for evaluating wetting phenomena on elemental mercury. A mercury spill in a mercury-wet porous media was simulated. The grid size was 30 by 1 by 90 cells (equivalent to 25x1x50m), with a grid refinement at the top part of the model, in order to achieve convergence during mercury infiltration. By using a Neumann boundary condition, elemental mercury infiltration was modeled, with a rate of 20 liter min^{-1}. In general, STOMP uses water-wet porous media as default. To do a rough calculation with mercury being the wetting phase, an analogue was done by changing water into mercury and vise versa. To do so, the density and viscosity of water had to be changed into that of elemental mercury, in the STOMP source code. In subroutine WATLQD, the density of water is defined and can easily be changed to the density of elemental mercury. Residual water saturations were set to 0, such that the initial wetting phase was set to 0 as well. Finally, the viscosity of the wetting phase (subroutine VISRL) was changed to that of elemental mercury in line 37444.

Scenario C: Fine sand with a loam lens. This scenario was used for illustrating the consequence of heterogeneity in a porous media. The grid size was 38 by 1 by 100 cells (equivalent to 25x1x50m), in order to achieve numerical convergence. A Dirichlet boundary condition was used for modeling DNAPL infiltration.

Scenario D: Fine sand with a (fractured) loam layer. This scenario was used to illustrate the effect of preferential flow through a fractured loam. The grid size was 25 by 1 by 50 cells (equivalent to 25x1x50m). A Neumann boundary condition was used for DNAPL infiltration with an infiltration rate of 50 liter min^{-1} over 1m² surface. This was done as a simplification of the Dirichlet boundary condition which did not yield convergence easily. This was a consequence of the high pressure boundary condition of 90cm equivalent elemental mercury. The loam layer was present at a depth of 5 meters and is 1m thick. In the case of a fractured zone it was implemented as a zone of 1m³ in the loam layer at X=12 to 13 meter.

Scenario E: Coarse sand and fine sand layer in the unsaturated zone (fig. 3B). This scenario was used to determine the influence of heterogeneities in the unsaturated zone and compared to the known PCE behaviour, according to Hofstee *et al*., 1998.

Scenario F: homogeneous medium sand with an unsaturated zone (fig. 4A, right figure). This scenario was used to determine the influence of the capillary fringe on elemental mercury migration. The model was seized 25x1x50cells (25x1x50 meter), with the water table at 10m depth.

3.2 Spatial moments

To quantify DNAPL plumes and its migration over time, spatial moments were used. It is an integration method to obtain statistical data on the centre of mass and its variance (Kueper and Frind 1991; French *et al*., 2000). By determining the vertical- and horizontal spreading, the shape of the plume could be expressed as a number, enabling comparison between multiple DNAPL plumes. The horizontal distribution of NAPL saturation, assumed to be a Gaussian function, was quantified by horizontal variance (i.e. parallel to the X-axis). The vertical spreading was described by the depth of the centre of mass, indicating the penetration depth. The integrals were numerically solved by using computational language FORTRAN 90. The integrals were determined by adding the NAPL saturation over the whole 2D-grid, assuming the midpoint of each grid to be representative for the whole grid. In the end, this resulted in the horizontal variance and depth of the centre of mass for each time step calculated by STOMP.

In this research, time periods needed to reach steady-state were determined by using the centre of mass. When the centre of mass changed less than 1% over 5 hours it was considered steady state, even though the plume was still slowly migrating (appendix B; fig. B6). This was done to obtain a time framework for all models, since some plumes continue migrating until infinite and therefore will not reach steady state.

Spatial moments, based on the integration of mass over two dimensions, is based on three moments. The first moment is the cumulative mass: M_{00}, the second and third moments are a proxy for centre of mass and the variance, respectively. The latter two are direction dependent, either in the X or Z-direction. The moments are given by:

$$M_{ij} = \phi \int_{-\infty}^{\infty} \int_{-\infty}^{\infty} S_{napl}(x, y)\, x^i z^j dx dz$$

where *i* and *j* denote the direction and the moment (e.g. M_{20} is moment two in the X-direction), φ is the porosity and S_{NAPL} the NAPL saturation. The centre of mass in the Z-direction and the variance in the X-direction are given by:

$$x_z = \frac{M_{01}}{M_{00}}$$

$$\sigma_x^2 = \frac{M_{20}}{M_{00}} - x_c^2$$

where x_z is the centre of mass in the Z-direction in [m], σ_x^2 is the variance in the X-direction [m²] and σ_x is the standard deviation in the X-direction [m].

3.3 Residual mercury saturation in the vicinity of a chlor-alkali-plant

During probing in the vicinity of a chlor-alkali-plant, a camera in the probe was used to visualize characteristics of the soil. The camera has a resolution of 1200x1600 and captures an area of 12x18mm (Deltares). As a result a rather high resolution depth profile of in-situ photos, to 9m depth was made, from which several pictures were used during this research.

Photos taken were used to obtain an idea on volumetric mercury content and its behaviour in a real soil. The pixels representing elemental mercury were used as a proxy for its volumetric content. Open source software R was used, in which the EBimage package was downloaded (www.bioconductor.org). This image processing software is capable of recognizing distinctive features in photos. Opening and closing procedures were used to determine the presence of mercury in each pixel; this was stored in a unit matrix I_{Hg} with '1' being mercury and '0' being no mercury (Pau *et al*., 2010; Appendix F). Then the volumetric mercury content (θ_{Hg}) could be determined by using:

$$\theta_{Hg} = \frac{\sum_{y=0}^{y=1200} \sum_{x=0}^{x=1600} I_{Hg}(x,y)}{1200 \times 1600}$$

which simply adds all the pixels containing mercury and divide them by the total amount of pixels in the photo. An idea about residual mercury saturation could then be determined by using:

$$S_{Hg} = \frac{\theta_{Hg}}{\phi}$$

In the end, these results were used to establish a model for elemental mercury in the subsurface.

Chapter 4: Parameters

This section describes all parameters used in this research, such as liquid, soil and hydrological parameters. Knowledge and data on elemental mercury in porous media is lacking, therefore scaling methods are used to obtain a reasonable amount of data and in the meantime to validate those common used scaling methods.

4.1 Fluid properties

Elemental mercury is known for its high viscosity, density and surface tension, compared to both PCE and water (table 4). To distinguish the behaviour of elemental mercury compared to other DNAPLs, PCE is used as a reference liquid. The interfacial tension, viscosity and density are considered to be constant throughout this research, except when they are tested on their sensitivity.

	PCE	*Elemental mercury*	*Water*	*Reference*
Interfacial tension				
water [dynes cm^{-1}]	44.4	375	-	Hofstee *et al*, 1998; Wilkinson, 1987
to air [dynes cm^{-1}]	32.6	485	72	Hofstee *et al*, 1998; Wilkinson, 1987
Density [kg m^{-3}]	1630	13500	1000	Devasena and Nambi, 2010
Viscosity [10^{-3} Pa· S]	0.89	1.554	1.00	Devasena and Nambi, 2010

Table 4: fluid properties used for multi-phase-flow model (PCE, elemental mercury and water).

4.2 Soil parameters

Soil properties are kept constant in order to maintain consistency in the results and to allow comparison between multiple scenarios. Therefore the relative permeability function, hydraulic conductivity, porosity and bulk density are kept constant for the four different soil types. Data for Crozier Loam originates from Busby *et al.*, 1995, for fine sand from Ippisch *et al*., 2006 and for coarse and medium sand from Devasena and Nambi, 2010 (table 5). The retention curve for coarse and medium sand is scaled back from the PCE-water Pc(S) curves, since no retention curve was determined during this experiment. Scaling is done by correcting the Pc(S) curve for PCE-water, described by the van Genuchten model, with the scaling factor (Lenhard and Parker, 1987b; Lenhard, 1994). By using the following scaling method,

$$P_c^{aw}(s) = P_c^{ow}(s) \times \beta_{ow}$$

the retention curve could be determined, with $\beta_{ow} = 1.6$ for PCE-water (Mayer and Hassanizadeh, 2005). Van Genuchten parameters obtained are α=0.32, n=4.3 and α=0.26 and n=5.8 for medium and coarse sand, respectively. The Pc(S) curve for medium and coarse sand are both similar to that of typical sand, with van Genuchten parameters of α=0.145 and n=2.68 (Mayer and Hassanizadeh, 2005).

The retention curve for fine sand has a higher entry pressure than for both coarse and medium sand, which is the expected difference in these curves. Next, the van Genuchten parameters for Crozier Loam are α=0.009, n=1.38 and has a larger entry pressure than any other soil type used in this research, these parameters correspond with typical values for loam, but inhibits higher entry pressure: α=0.036 n=1.56 (Mayer and Hassanizadeh, 2005).

The relative permeability is determined by using Mualem's model, due to the limitations in range of n in Burdines model (Mualem n>1 and Burdine n>2, with n being a fitting parameter in the van Genuchten function).

	Unit	*Coarse Sand*	*Medium Sand*	*Fine Sand*	*Crozier Loam*
Porosity	-	0.33[(1)]	0.33[(1)]	0.43[(2)]	0.41[(2)]
Quartz density	Kg m^{-3}	2650	2650	2650	2650
Tortuosity		Millington and Quirk	Millington and Quirk	Millington and Quirk	Millington and Quirk
Hydraulic conductivity	Cm min^{-1}	150[(3)]	120[(3)]	80[(3)]	0.21 [(4)]
Relative permeability		Mualem	Mualem	Mualem	Mualem
α	cm^{-1}	0.26[(1)]	0.32[(1)]	0.024[(5)]	0.009[(6)]
n	-	5.8[(1)]	4,3[(1)]	4.4[(5)]	1.38[(6)]

Table 5: Soil properties for 4 artificial porous media: Coarse sand, Medium sand, Fine sand and Crozier loam. 1) Data according to Devasena and Nambi, 2010, with the van Genuchten parameters scaled according to Lenhard and Parker 1987B. 2) Data according to Mayer and Hassanizadeh, 2005. 3) Assumed hydraulic conductivities, relative differences according to Mayer and Hassanizadeh, 2005; table 3.1 pp. 48. 4) Data according to van Genuchten, 1980. 5) Data according to Ippisch et al, 2006 and 6) Data according to Busby et al., 1995.

4.3 Pc(S) curves for elemental mercury and PCE

Current multi-phase-flow models for NAPLs apply Leverett scaling to obtain NAPL-water and NAPL-air Pc(S) curves. However, the applicability of Leverett scaling on elemental mercury has to be evaluated. By using PCE-water and mercury-water Pc(S) curves from one experimental research, PCE-water Pc(S) curve can be cross scaled to mercury-water Pc(S) curve, which can be checked for its validity. The retention curve for medium and coarse sand is determined in the previous section. This can be up-scaled to mercury-water Pc(S) curves and then compared to measured parameters. Up-scaling is done by using:

$$P_c^{mw}(s) = \frac{P_c^{aw}(s)}{\beta_{mw}}$$

where β_{mw} is the scaling factor for mercury-water. The reference interfacial tension used in this scaling factor is either 72 dynes cm^{-1} or 860 dynes cm^{-1}, hence the surface tension of water or the sum of interfacial tension for mercury (Lenhard, 1994). Consequently, β_{mw} is either 0.192 or 2.29, from which 0.192 seems most reasonable since it increases the entry pressure from a water-air system to mercury-air. The measured entry-pressure for mercury-water is 18.5 and 29cm of water head for coarse and medium sand, respectively, whereas Leverett-scaled van Genuchten parameters, derived from PCE-water measurements, have an entry-pressure of 10.7cm and 9.5cm water head, respectively (fig. 5A). However, when comparing measured entry-pressures with scaled entry-pressures on basis of its grain size, the scaled entry-pressures appears to be reasonable, indicating a deviation of Leverett-scaling via PCE-water experiments within the same article by Devasena and Nambi, 2010 (section 2.4). Moreover, the van Genuchten parameters for elemental mercury in saturated medium sand, from the aforementioned article, implies a too high entry-pressure of 70-80cm, compared to the measured 29cm. Scaled Pc(S) curves for medium and coarse sand within one model is not used, such that coarse sand, which yields an artificial higher entry pressure than medium sand, is not falsely compared. In the end, the entry pressure for elemental mercury becomes higher from fine sand to either coarse or medium sand.

For sake of illustration, a less-permeable layer is modelled to illustrate the influence of heterogeneities. This is done by up-scaling a retention curve of Crozier Loam, with a slightly different reference interfacial tension, due to the use of less-permeable porous media. Busby et al. (1995) conducted an experiment to determine β and the Pc(S) curve of TCE in saturated soils to illustrate the correctness of Leverett-scaling. In the aforementioned research Crozier loam was used as a less permeable porous media. This data is used in this research to determine a reference interfacial tension for Crozier loam by using:

$$\sigma^* = \beta_{tw} \times \sigma_{tw}$$

where *tw* denotes TCE-water. This results in a reference interfacial tension of 97.6 dynes cm^{-1}. Consequently, β becomes higher for this new reference interfacial tension than for using the default 72 dynes cm^{-1}. The Leverett-scaled Pc(S) curve for fine sand and Crozier loam are given in table 6 and plotted in figure 5B, which illustrates a pronounced higher Pc(S) curve for Crozier loam, with the exception at high water saturation. Therefore the Brooks-Corey function is used to determine the difference between Brooks-Corey and van

Genuchten function for DNAPL infiltration in Crozier loam (h_e=35cm, λ=0.24 and β=0.192).

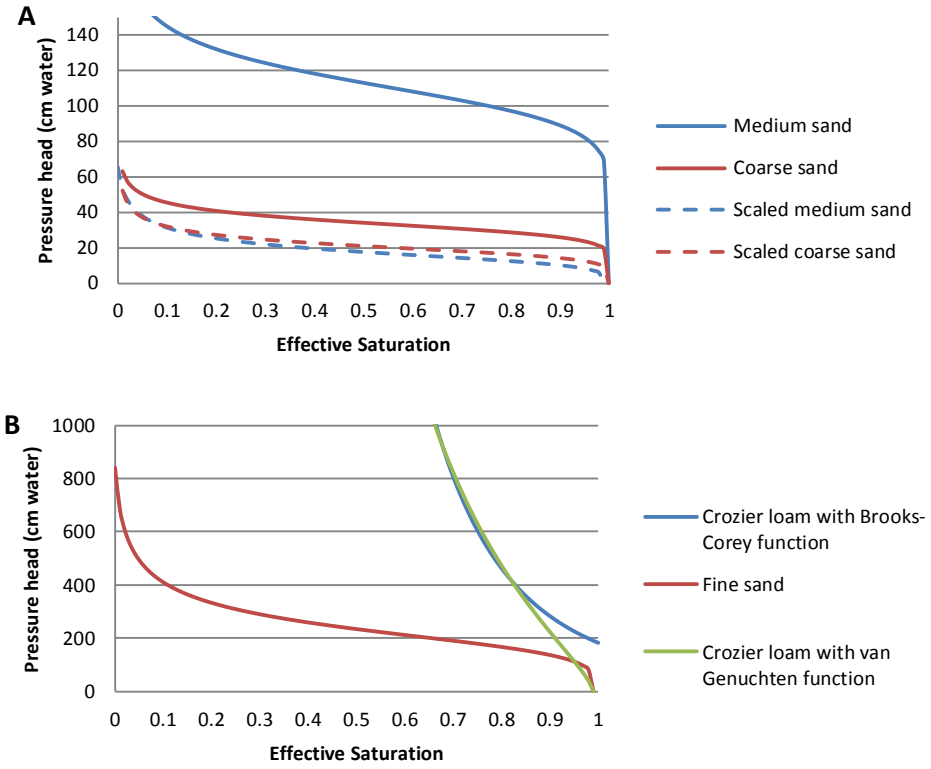

Fig. 5: Pc(S) curves for elemental mercury in different saturated soils. A) Measured mercury-water Pc(S) curves for medium and coarse sand, along with the Leverett- scaled Pc(S) curves derived from PCE-water curves. Medium sand Pc(S) curve by Devasena and Nambi does not correspond with the in the article mentioned entry-pressure. B) Pc(S) curves for fine sand and Crozier loam for elemental mercury in water.

	PCE				*Elemental mercury*				
	α	n	β	σ^*	α	n	β	σ^*	Reference
Coarse Sand	0.16	5.8	1	44.4	0.03	8.2	1	375	Devasena and Nambi, 2010
Medium Sand	0.2	4.3	1	44.4	0.009	9.4	1	375	Devasena and Nambi, 2010
Fine Sand	0.024	4.4	1.6	72	0.024	4.4	0.192	72	Ippisch *et al*., 2006
Crozier Loam	0.009	1.38	2.2	97.6	0.009	1.38	0.26	97.6	Busby *et al*, 1995

Table 6: van Genuchten parameters, scaling factors and reference interfacial tensions used for Pc(S) curves.

4.4 Residual saturations

Residual saturation for elemental mercury is known for medium and coarse sand. To establish a scaled residual saturation for fine sand and Crozier Loam, data on PCE is used. The known ratio between residual saturation of PCE and elemental mercury in medium sand is linear extrapolated to fine sand or Crozier loam, by using known residual saturation for PCE in the according soil, according to:

$$S_1^{Hg} = S_1^{PCE} \frac{S_2^{Hg}}{S_2^{PCE}}$$

where S_1^{Hg} is the residual saturation of elemental mercury in soil 1, S_1^{PCE} is the known residual saturation of PCE in soil 1 and 2 denotes the known residual saturations (table 7).

	PCE		*Elemental mercury*		
	Sirw	Srn	Sirw	Srn	Reference
Coarse Sand	0,163	0,168	0,07	0,04	Devasena and Nambi, 2010
Medium Sand	0,288	0,275	0,1	0,08	Devasena and Nambi, 2010
Fine Sand	0,045*	0,17	0,045*	0,049**	Mayer and Hassanizadeh, 2005
Crozier Loam	0,095*	0,13	0,095*	0,014**	Mayer and Hassanizadeh, 2005

Table 7: residual- and irreducible water saturations for PCE and elemental mercury were used in this research. Residual saturations of elemental mercury for Fine sand and Crozier loam, were linear extrapolated from known residual saturations in the case of PCE.

4.5 Three-phase-flow

This research gives a preliminary reasoning on the behaviour of elemental mercury in the vadose zone, by modelling results obtained by Hofstee *et al.*, 1998. Parameters are derived from this article to compare the behaviour of the well known DNAPL PCE to that of elemental mercury. Data is represented in table 8. Van Genuchten parameters are used instead of Brooks-Corey parameters to maintain correspondence between the other model scenarios. Elemental mercury and PCE are non-spreading DNAPLs but were modelled as spreading DNAPLs.

Parameter	*Coarse-grained*	*Fine-grained*
Porosity	0.349	0.406
Sirw	0.035	0.038
Srn	0.042	0.051
Permeability (m^2)	$72.3x10^{-12}$	$2.1x10^{-12}$

Table 8: Model parameters for PCE, used in this report for three-phase-flow (Hofstee et al., 1998).

4.6 Fractured media

In order to evaluate the behaviour of elemental mercury, a model containing fractured porous media is done, such that preferential flow occurs. A rather impermeable Crozier loam layer in fine sand is modelled, which contains a fractured zone. This is done by using the dual-porosity model application in STOMP, which is capable to model a fractured zone consisting of a fault gauge matrix and original media. In this model, it is assumed that the hydraulic conductivity of the fault matrix is arbitrarily set 100 times higher than that of Crozier loam. In literature this factor is even higher (from 1.05 to 2000 cm d^{-1} ;Simunek *et al*., 2003). For simplification, the Pc(S) curve is kept constant, implying an underestimation of preferential flow through the fractured Crozier loam, since the entry pressure is higher than it should be in the fractured media. The characteristic length is 0.5 (Simunek *et al*., 2003). The model is used for both PCE and elemental mercury and for fractured loam and intact loam, such that the differences and processes become clear.

Chapter 5: Results

5.1 Saturated homogeneous medium sand

To study the behaviour of elemental mercury in porous media, a spill was modeled in saturated homogeneous medium sand. First, the migration of elemental mercury was compared to that of PCE. Next, a sensitivity analyses was done on elemental mercury by changing its density and viscosity to that of PCE and by changing the residual saturation of PCE to that of elemental mercury. Finally, the consequence of elemental mercury as non-wetting fluid was determined by modeling a mercury-wet porous media. Results are reported for final distributions in spatial moments and figures, whereas flow processes are reported solely in the evolvement of spatial moments over time.

5.1.1 Elemental mercury and PCE

Elemental mercury and PCE were modeled in a saturated homogeneous medium sand, to establish fundamental difference in the behaviour between these two DNAPLs in a saturated zone (*scenario A*; fig. 6). Results indicated that elemental mercury has a higher infiltration depth than PCE, 32m and 11m, respectively. This was supported by the spatial moments for the final distribution, which indicated that the center of mass was located deeper for elemental mercury than for PCE, 11.65m and 3.63m, respectively (fig. 7). Moreover, the center of mass for both DNAPLs was located in the upper part of the plume. The horizontal variance of PCE was larger than that of elemental mercury (2.33m² and 1.36m², respectively; fig. 7), which was a consequence of the large horizontal size of the PCE plume. Due to the high entry-pressure for both DNAPLs, equivalent to 90cm mercury head, PCE spread horizontally just beneath the top model boundary. To check this hypothesis, another model with an infiltration pressure equivalent to 90cm PCE head was done (Appendix C, fig. C1A). By changing the infiltration pressure, the horizontal spreading decreased and therefore the infiltration depth increased (horizontal spreading: 1.37m², depth center of mass: 5.6m, infiltration depth 16m). In summary, elemental mercury migrated deeper than PCE, whereas PCE had a higher horizontal variance, due to a high entry-pressure.

Elemental mercury required more time to reach entrapment than PCE, 20 and 5 hours, respectively. In the case of PCE with 90cm PCE head as infiltration head, it required 15hours to reach entrapment. Due to the low residual saturation, elemental mercury was able to infiltrate deeper than PCE, assuming the same volume of DNAPL spill for both elemental mercury and PCE. Consequently, it required more time for elemental mercury to reach entrapment. A quantification of flow velocity was not made due to the large influence of boundary conditions on PCE spreading.

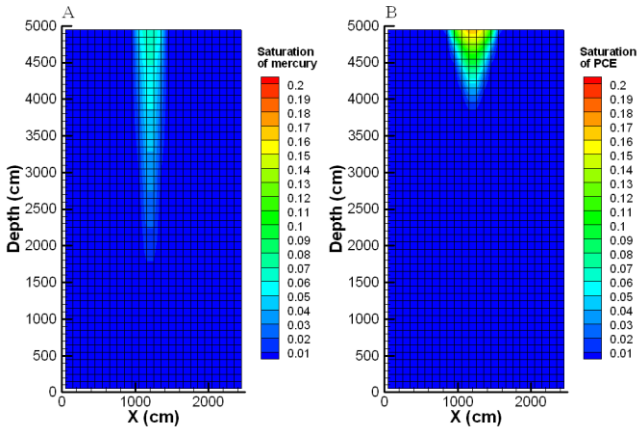

Fig. 6: DNAPL leakage in a saturated zone consisting of medium sand. A) Elemental mercury after t=70 hours, with V_{napl} = 1.38x10³L, and $t_{equilibrium}$=20 hours. B) PCE after t=70 hours, with V_{napl}=1.35x10³L and $t_{equilibrium}$=5 hours.

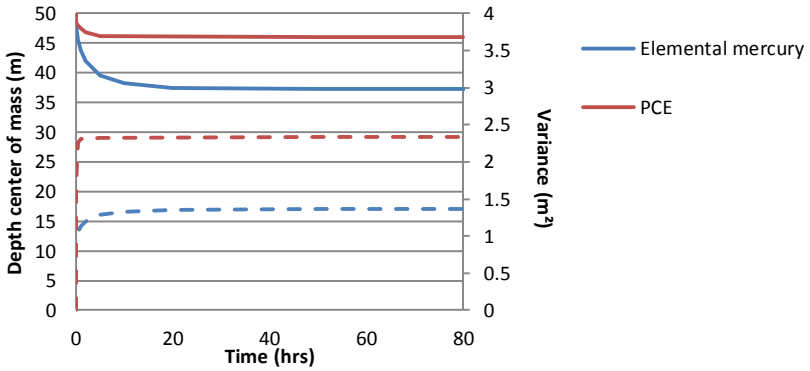

Fig.7: Spatial moments for PCE and elemental mercury in saturated homogeneous medium sand. Solid line indicated height above model bottom and the dotted line indicates horizontal variance. Elemental mercury infiltrates deeper and has lower horizontal spreading compared to PCE. With $t_{equilibrium}$= 5 hours and $_{equilibrium}$= 20 hours, for PCE and elemental mercury, respectively.

5.1.2 Influence of viscosity, density and residual saturation

The behaviour of elemental mercury is assumed to be dominated by its high density and capillary pressure, indicated by its capillary- and bond number (Devasena and Nambi, 2010). To make a distinction between the importance of density and viscosity, a sensitivity analyse was done in *scenario A*, by changing either density or viscosity to that of PCE (i.e. density from 13.500 kg m^{-3} to 1.630 kg m^{-3} and for the viscosity $1.554x10^{-3}$ Pa· s to $0.89x10^{-3}$ Pa· s). Moreover, PCE was given a residual saturation equal to that of elemental mercury to obtain the influence of the low residual saturation on migration. The results were compared to the original model for elemental mercury to obtain insight in the different importance of density, viscosity and residual saturation.

By decreasing the density of elemental mercury, the plume shape became distinctively different (fig. 8B). The deep migration, characterizing elemental mercury flow, was completely gone (depth of infiltration became 12.5m instead of 37.5m) and transferred to a higher horizontal variance: 3.55m² instead of 1.36m² (fig. 9). To achieve convergence in this model, the grid was refined towards the inlet of mercury, since the change in

parameters inhibits flow by taking out a major driving force (i.e. the density). This inhibition to flow was found in the time required to reach entrapment. This was 25hours when changing the density, compared to 20 hours for the original mercury plume.

Decreasing the viscosity of elemental mercury to the value of PCE had limited effect on mercury spreading, but allowed an insight into its influence on flow (fig. 8C). The shape of the plume slightly differed from the original mercury plume, its depth of the center of mass was 12.5m with a horizontal variance of 0.92m² (fig. 9). Even though the model with different viscosity contained slightly less mercury (8% less mercury), it achieved a higher infiltration depth than the reference case. Since viscosity is the resistance to flow, a lower viscosity enables flow to be faster than with a higher viscosity, hence mercury with a lower viscosity flows faster than with its original parameters (i.e. time required for entrapment was 15 hours, compared to 20 hours for original mercury).

To establish the influence of the low residual saturation on the final distribution of elemental mercury, a model was done with PCE. The low residual saturation was implemented in the model of PCE. The boundary condition was set on 90cm PCE head instead of 90cm mercury head, to minimalize the influence of boundary conditions. Results obtained indicated a similarity between the PCE plume and the plume of elemental mercury (fig.8D). This was illustrated by evolvement of spatial moments over time, which was the same for both models with the exception of mercury migrating faster than PCE (i.e. time required for entrapment was 20 and 35 hours, respectively; fig. 10).

In summary, migration of elemental mercury is governed by its density, whereas the viscosity slightly counteracts this flow. The low residual saturation is considered a main parameter governing its distribution, whereas density governs flow velocity.

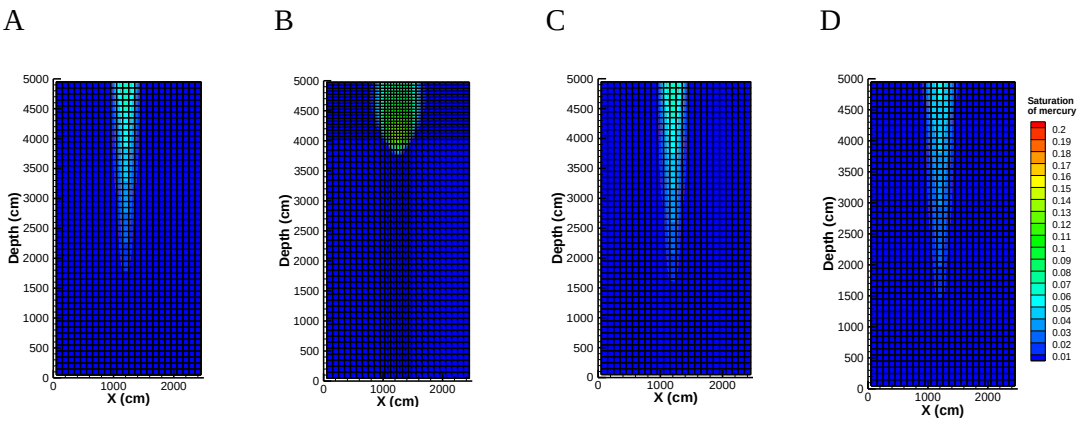

Fig.8: Elemental mercury and PCE leakage in a saturated zone, consisting of medium sand, for determining the influence of two particular parameters of mercury. A) Reference case with the original properties of mercury after t=20 hours, with V_{napl}=1.50x10³L and $t_{equilibrium}$=20 hour. B) Mercury with the viscosity of PCE after t=20 hours, with V_{napl}=1.38x10³L, and $t_{equilibrium}$=15 hours. C) Mercury with the density of PCE after t=20 hours with V_{napl}=2.09x10³L and $t_{equilibrium}$=25 hours. D) PCE with the residual saturation of elemental mercury and an entry-pressure equivalent to 90cm PCE head instead of 90cm elemental mercury, after t=80hours, V_{napl}=1.44x10³L and $t_{equilibrium}$≈ 35hours .

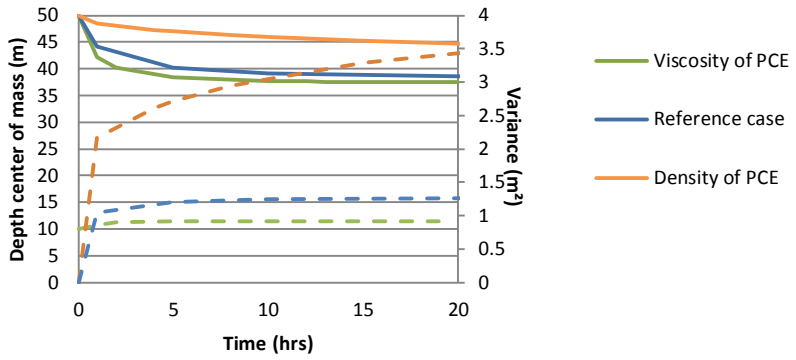

Fig.9: Spatial moments for a sensitivity analyses on elemental mercury in saturated homogeneous medium sand. Solid line indicated height above model bottom and the dotted line indicates horizontal variance. Elemental mercury with the original values (i.e. reference case), $t_{equilibrium}$ = 20 hours. Elemental mercury with the viscosity of PCE, $t_{equilibrium}$=15 hours. Elemental mercury with the density of PCE, $t_{equilibrium}$= 25 hours.

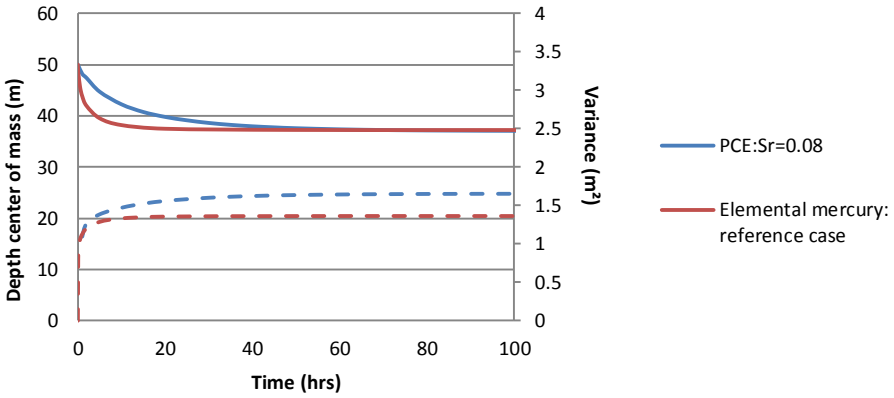

Fig.10 : Spatial moments for elemental mercury and PCE with the residual saturation of elemental mercury in a saturated homogeneous porous media. Solid line indicated height above model bottom and the dotted line indicates horizontal variance. With $t_{equilibrium}$=20hours for elemental mercury and $t_{equilibrium}$=35 hours for PCE.

5.1.3 Mercury wet porous media

Throughout this research elemental mercury was assumed to be non-wetting, even though mercury might be the wetting phase in certain types of soil, such as loam, clay or other organic-rich lithologies. To evaluate the difference in wettability, a quick adjustment was done in the source code to get a rough idea about the flow behaviour in a mercury wet porous media (*scenario B*).

Results obtained indicated a different flow regime compared to water-wet porous media in saturated homogeneous medium sand. The difference in flow behaviour was reflected in flow velocity and the shape of the plume (fig. 11). After 100 days the plume was still migrating towards the model bottom, whereas in a water-wet porous media mercury became entrapped after 20 hours. Time needed for mercury to reach the model bottom cannot be determined, since numerical dispersion and artificial mercury flow decreases model reliability (i.e. NAPL saturation at model bottom in figure 11C). Initially, the mercury

saturation in the model was $2.6x10^{-4}$, even though the minimum mercury saturation was put to 0.0. The quick assessment of the code did not result in perfect model runs, but merely in approximations. Moreover, no entrapment was modelled, enabling mercury to reach the bottom. Nevertheless, a mercury-wet porous media resulted in a slow mercury migration compared to a water-wet porous media. The centre of mass seemed to be located in the lower part of the plume, however a reliable quantification by spatial moments could not be made, due to artificial flow in the model. So, the main characteristics of a mercury-wet porous media upon mercury infiltration were the slow migration of mercury as a result of different wettability. Whereas the centre of mass, located towards the bottom of the plume, differs from mercury in water-wet porous media.

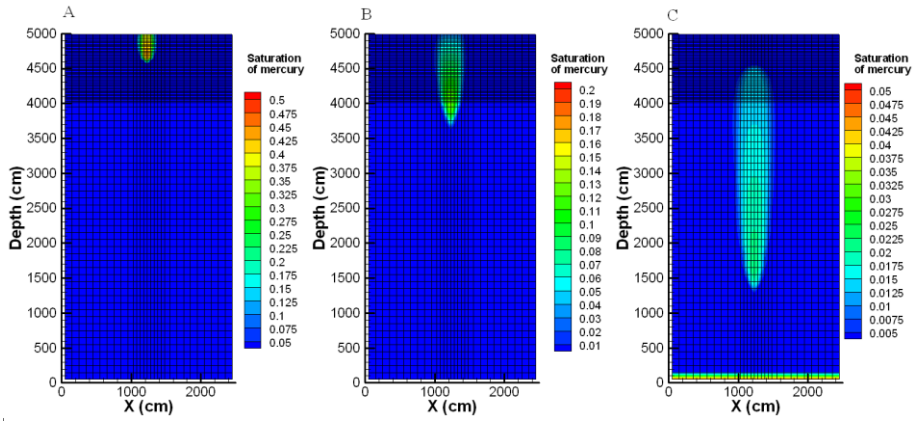

Fig.11: An elemental mercury leakage was modelled in a mercury-wet porous media. A volume of 1.12 m³ is infiltrated to the model by using a Neumann boundary condition, by a rate of 20 L min^{-1}. A) after 2hrs. B) after 20 hours. C)after 100 days, with an artificial mercury accumulation at the model bottom.

5.2 Saturated heterogeneous porous media

In soil and groundwater systems heterogeneities occur naturally and influence the migration of DNAPLs. To establish the difference between PCE and elemental mercury in heterogeneous porous media, three heterogeneities were modelled with fine sand and Crozier Loam, including a loam lens, loam layer and a fractured loam layer.

5.2.1 Fine sand with a loam lens

A model with a loam lens in fine sand (*scenario C*) was used to compare the behaviour of elemental mercury with that of PCE in a simple heterogeneity. The results obtained indicated some major differences in flow behaviour. But a striking similarity between PCE and elemental mercury was present as well (fig. 12).

5 Times the volume of mercury was required for PCE to accumulate at the loam lens. This was due to the horizontal spreading of PCE as a consequence of the high infiltration pressure, as indicated in paragraph 5.1.1. Therefore the horizontal variance of PCE was small compared to that of elemental mercury (3.48m² for mercury and 3.04m² for PCE; Appendix B: fig. B2). The large horizontal variance for elemental mercury originated from the spreading at the loam lens, whereas the horizontal spreading for PCE at the loam lens was comparable to that at the surface, hence decreasing the horizontal variance at the loam lens. The overflow of DNAPL over the lens-edges is similar shaped for both mercury and PCE. Therefore, the horizontal spreading of elemental mercury and PCE was similar during flow over the heterogeneity. Elemental mercury infiltrated deeper in porous media than PCE, even though the volume of PCE was 5 times higher. The depth of the centre of mass was for elemental mercury around the Crozier loam lens, whereas for PCE it was in between the top and the loam lens (12.8 m and 5.5 m, respectively). Indicating the deeper infiltration of elemental mercury compared to that of PCE. Moreover, PCE required slightly more time to reach steady state than elemental mercury (i.e. 30 hours and 25 hours, respectively). So, elemental mercury and PCE did flow via preferential pathways, hence over the edges of the lens. Elemental mercury infiltrated deeper and faster than PCE. Infiltration of elemental mercury in the Crozier loam lens will be evaluated in the following paragraph.

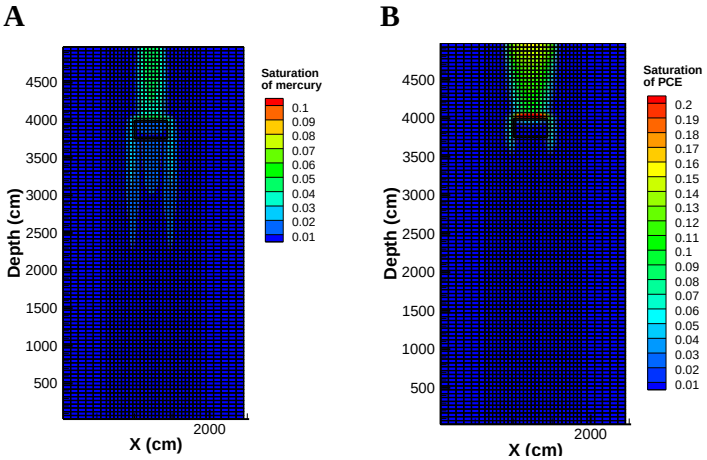

Fig. 12: DNAPL leakage in a fine sand model, with a loam lens indicated by the black-box. This is to illustrate the effect of heterogeneities on multi-phase-flow. A) Elemental mercury, V_{napl} =1.46 m³ and $t_{equilibrium}$=25 hours. B) PCE, V_{napl}=3.1 m³ and $t_{equilibrium}$=30 hours.

5.2.2 Fine sand with a (fractured) loam layer

Fractured porous media enhances preferential flow of a DNAPL in the subsurface, such that impermeable layers become permeable. This would allow flow through impermeable layers, such as clay, loam or solid rock. In order to illustrate the behaviour of elemental mercury in a preferential flow, a model was used with a fractured loam layer in fine sand (*scenario D*). This was compared with the same model without fractures, for both mercury and PCE.

Elemental mercury and PCE showed the same features in the case of an intact loam layer, horizontal spreading at the interface and infiltration in the loam layer (fig. 13A and fig. 13C). As a consequence of the initial impermeable loam layer, both DNAPLs tended to spread at the interface, from which elemental mercury spread the most (horizontal variance is 6.91m² and 3.40m² for elemental mercury and PCE, respectively). Moreover, PCE tended to accumulate in height rather than spreading horizontally on top of the loam layer, whereas mercury tended to spread horizontally rather than to accumulate on top of the loam layer. Time required to reach a steady-state situation was equal for both DNAPLs and was 10 hours. Infiltration through the loam layer was present for both DNAPLs, after DNAPL had accumulated at the loam layer. In *scenario C* and *scenario D* (the loam lens and loam layer or fig. 12A and fig. 13A, respectively): elemental mercury infiltrates Crozier Loam, under low saturations (i.e. 0.01 to 0.02). This might be either true or a numerical error in the Pc(S) curve (paragraph 4.3), which has a higher capillary pressure for fine sand than Crozier Loam at low NAPL saturations. To make this distinction, a model run with fine sand and a Crozier loam layer was done (*scenario D*), including Brooks-Corey Pc(S) curves rather than van Genuchten function. In this manner, the entry-pressure for Crozier loam is distinctively larger than for fine sand. Results indicated that elemental mercury infiltrated Crozier Loam, despite of the Brooks-Corey function (fig. 13E). Therefore, infiltration of elemental mercury found in figure 12 and 13 seems to be true and there is no numerical problem with the Pc(S) curve.

The presence of a fractured zone in the loam layer resulted in a preferential flow, rather than DNAPL infiltrating into the loam layer. This reduces the horizontal spreading for both DNAPLs at the interface and inhibited infiltration in the loam layer (horizontal variance was 2.26m² and 1.94m² for elemental mercury and PCE, respectively). The fractured zone acted as a preferential pathway for DNAPL and reduces accumulation at top of the lithology interface. Residual saturations in the fractured zone was put on 0, therefore no entrapment occurred at the fractured zone. A plume developed below the loam layer, which was expected for both DNAPLs. It extended deeper than without a loam layer, indicating the effective transport via fractured porous media (for elemental mercury: 37m in the case of a fractured loam and 32m in the case of no loam layer at all; fig 6A, with a loam layer of 2m thick). Moreover, it took more time for elemental mercury to reach steady-state than in the case of an intact loam layer (i.e. 30 hours and 35 hours for elemental mercury and PCE, respectively). In summary, preferential flow through the fractured loam is similar for both DNAPLs whereas both DNAPLs infiltrated an intact loam layer.

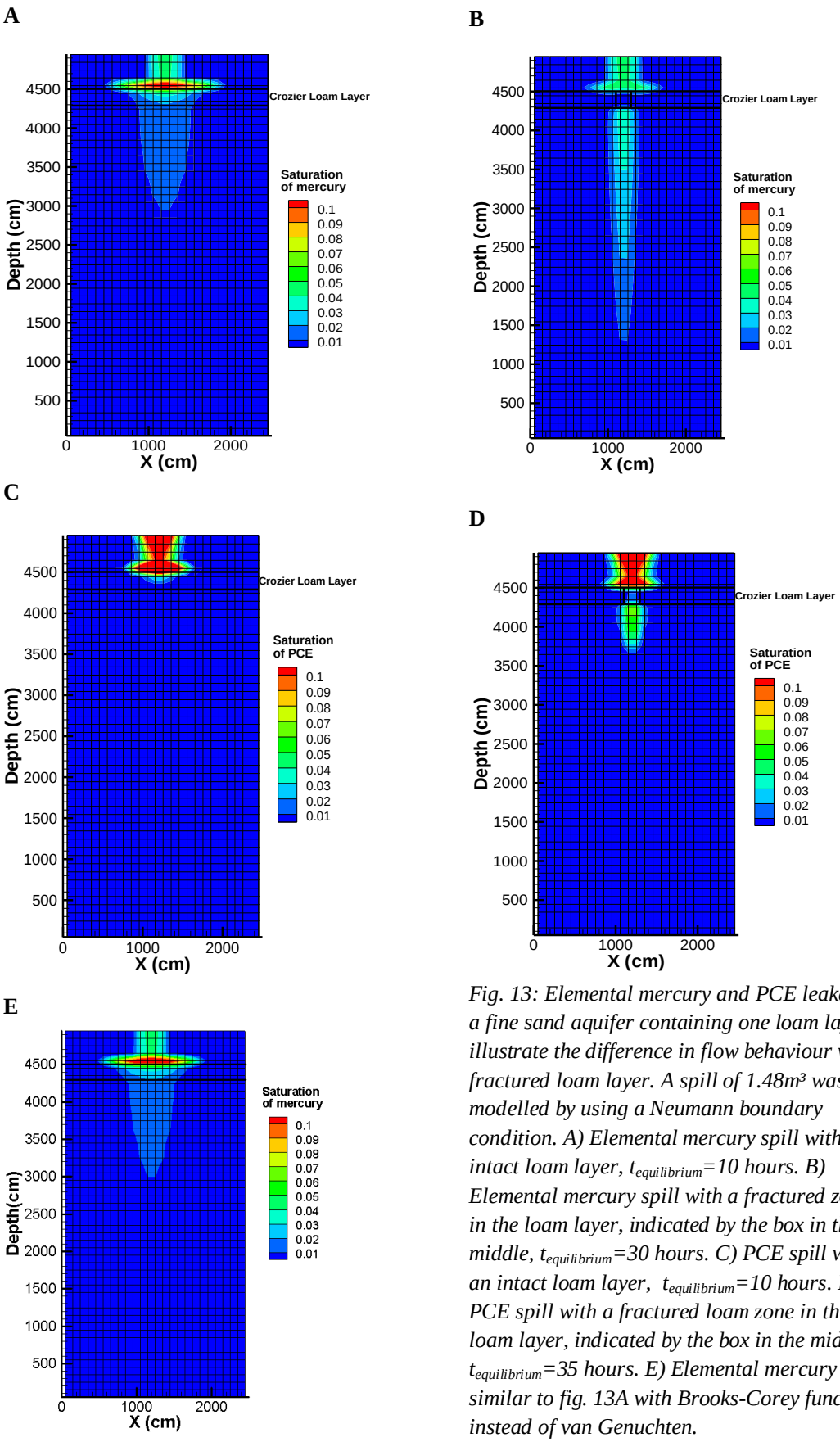

Fig. 13: Elemental mercury and PCE leakage in a fine sand aquifer containing one loam layer to illustrate the difference in flow behaviour with a fractured loam layer. A spill of 1.48m³ was modelled by using a Neumann boundary condition. A) Elemental mercury spill with an intact loam layer, $t_{equilibrium}$=10 hours. B) Elemental mercury spill with a fractured zone in the loam layer, indicated by the box in the middle, $t_{equilibrium}$=30 hours. C) PCE spill with an intact loam layer, $t_{equilibrium}$=10 hours. D) PCE spill with a fractured loam zone in the loam layer, indicated by the box in the middle, $t_{equilibrium}$=35 hours. E) Elemental mercury similar to fig. 13A with Brooks-Corey function instead of van Genuchten.

5.3 Three-phase flow

To establish a first order insight in mercury migration through the unsaturated zone, a model run similar to the article by Hofstee *et al*., 1998 was done for elemental mercury (*scenario E*). In the aforementioned article, it seems that models were able to predict the initial behaviour of PCE but not the final distribution, since the models are based on spreading NAPLs and PCE is a non-spreading DNAPL. Therefore, modelling mercury as a spreading-liquid is thought to be representative for processes during flow and not for determining final distributions. In this manner, the infiltration of elemental mercury in an unsaturated heterogeneous porous media can be studied. First, the case of PCE was simulated to obtain the same results as for a spreading DNAPL in the article by Hofstee *et al*., 1998. The model indicated for PCE to accumulate at the bottom of the fine sand layer, which is in contrast to experimentally obtained data, hence mercury accumulates in the upper part of the fine layer (fig. 14A). However, PCE did infiltrate a partially saturated fine sand heterogeneity.

Implementing elemental mercury in the model resulted in remarkable features, assuming Leverett scaling to apply. After infiltration of 650ml mercury, it spread on the interface between coarse and fine sand until it reached the model boundaries, which resulted in an increasing head (fig. 14B). In this manner, the entry-pressure of fine sand was overcome and mercury infiltrated into the fine sand layer. It became entrapped at the upper part of the fine sand (fig. 14C). So the entry-pressure of fine sand was exceeded when horizontal spreading is not infinite. This is not comparable with PCE as a DNAPL, since both spreading and non-spreading PCE infiltrate into the fine sand without reaching model boundaries (Hofstee *et al*., 1998).

To illustrate the behaviour of elemental mercury at the water table and capillary fringe, a model run was done, in a phreatic aquifer, consisting out of homogeneous medium sand (fig. 15; *scenario F*). The model solely simulates an intermediate and spreading DNAPL. Consequently, the model indicated barely any entrapment in the unsaturated zone and a familiar plume in the saturated zone. Mercury in the saturated zone showed the same particular features as in previous models (fig. 6A). At the water table no accumulation was present, indicating the low influence of the capillary fringe on mercury migration. Moreover, the horizontal size of the plume decreased from the unsaturated to the saturated zone. In summary, the water table and capillary fringe show limited effect on an intermediate wetting and spreading elemental mercury.

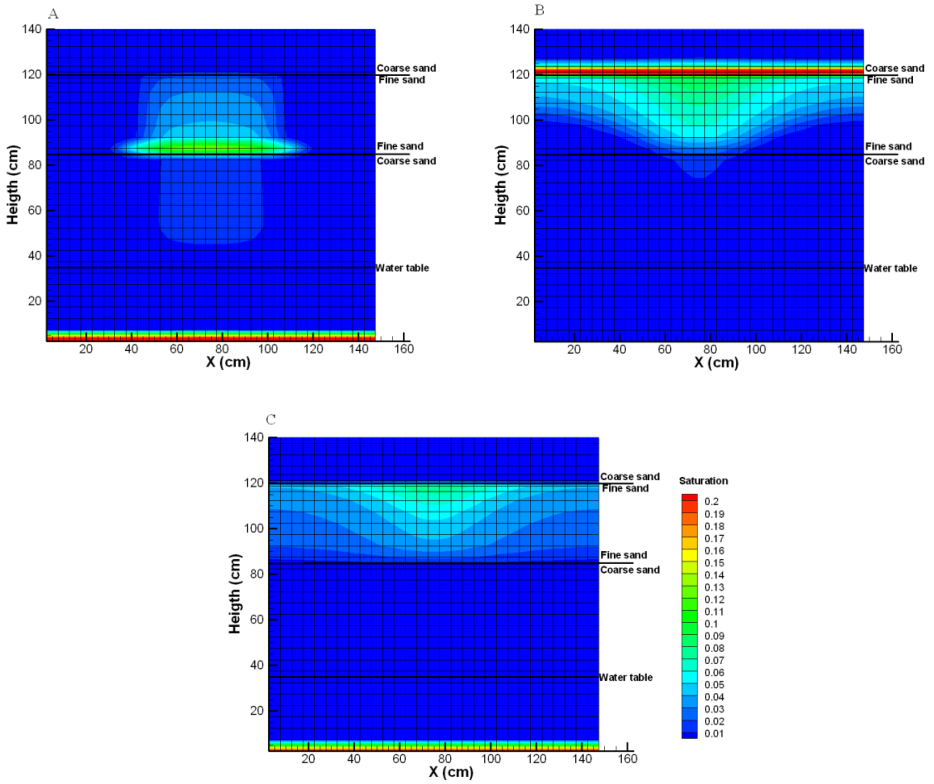

Fig. 14: DNAPL spill in the unsaturated zone, model according to Hofstee et al.*, 1998. The model consists of coarse sand with a fine sand layer. A) PCE after 3.5 days, B) elemental mercury after 1hr and C) elemental mercury after 3.5 days.*

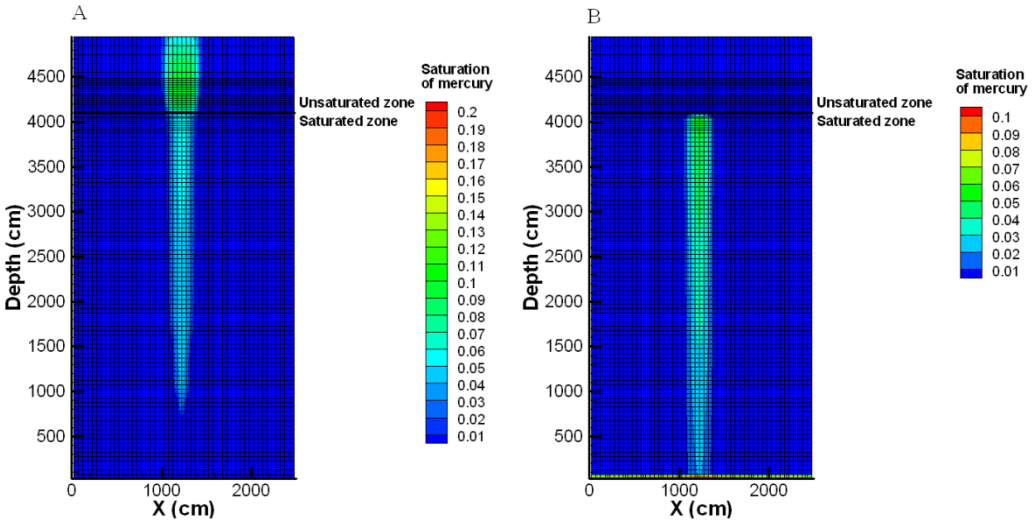

Fig. 15: Elemental mercury spill in a phreatic aquifer, for illustring processes at the capillary fringe. Mercury is modelled as a spreading DNAPL with entrapment, with V_{napl} *= 2.0m³. A) after 10 hours and B) after 100 days.*

5.4 Residual mercury in the vicinity of a chlor-alkali-plant

During a probing session in the vicinity of a chlor-alkali plant, soil photos were taken from within the probe itself. These photos visualized the subsurface by a vertical profile of multiple photos, taken every 1cm, where one photo was sized 12 by 18mm of soil (1200 by 1600 pixels). In-situ elemental mercury was visualized with this process, whereas the presence of elemental mercury on this site was also established with other field-observations at the surface. Probing was done up to a depth of 9m, where elemental mercury was present at the deepest observed depth. Elemental mercury visualized on the photos was used as a proxy for the volumetric content. However, residual mercury found in the soil is not necessarily the correct mercury content. Preferential flow or smearing of mercury to the glass plate in front of the camera might occur, due to a small gap between the soil and the probe. The size of a photo is 12x18mm which is supposed to be larger than the representative elementary volume (REV), otherwise the volumetric content found on a single photo would not represent the true-average of a soil sample. Moreover, in-situ elemental mercury is subjected to chemical processes occurring in soils, such as dissolution and chemical reaction, which may decrease the volumetric mercury content. This implies that the volumetric content found is not the initial volumetric content, which is found in multi-phase-flow models, but a later stage volumetric content. Thus, the mercury found by analyzing in-situ photos is merely an indication for the volumetric content of mercury.

Elemental mercury was present as disconnected blobs with sizes up to 1mm, which were heterogeneous distributed (fig. 16). In general, elemental mercury was more visually present in sandy layers than other lithologies. This, however, might be due to untraceable small blobs in finer porous media (i.e. blobs smaller than one pixel). Volumetric mercury contents obtained ranges from 0.016 to 0.089 or a residual saturation of 0.05 to 0.30, respectively (assuming a porosity of 0.33; table 7). The mercury content could solely be determined for sandy soils, since other lithologies showed too much heterogeneity within one photo for the method to apply. In summary, elemental mercury was found as a DNAPL in the vicinity of a chlor-alkali plant to at least 9m depth, from which some data on volumetric content is present.

Depth (m)	*Soil type*	*Depth sample (m)*	*Volumetric mercury content*	*Residual saturation*
1.00-1.20	Sandy layer	1.18	0.04083	0.12
2.88-3.00	Sandy layer	-	-	-
3.50-3.63	Sandy layer	3.53	0.09993	0.30
3.92-4.15	Sandy layer	4.00	0.04249	0.13
4.79-5.48	Sandy layer	4.81	0.025	0.08
6.33-6.51	Sandy layer	6.34	0.025	0.08
6.75-6.96	Sandy layer	6.87	0.053	0.16
7.44-7.69	Sandy layer	7.57	0.030	0.09
8.12-8.19	Sandy layer	8.13	0.07223	0.22
8.32-8.81	Sandy layer	8.63	0.01657	0.05

Table 7: Volumetric mercury content extracted from probing data, by using image processing software. Probing is done in the vicinity of a chlor-alkali-plant. Residual saturation is determined by assuming porosity to be 0.33.

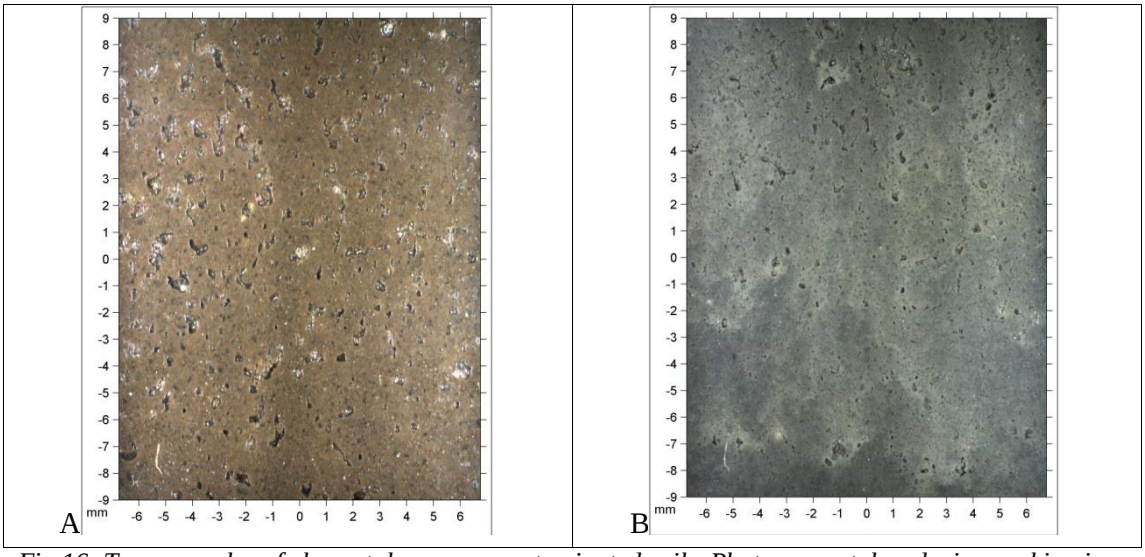

Fig.16: Two examples of elemental mercury contaminated soils. Photos were taken during probing in the vicinity of a chlor-alkali-plant, in a sandy soil. A) at 8.130m depth, volumetric mercury content 0.073 and B) at 6.34m depth, volumetric mercury content of 0.025.

Chapter 6: Discussion

6.1 Elemental mercury in the saturated zone

6.1.1 Assumptions

Elemental mercury is considered a non-wetting DNAPL, given its immiscibility and high density. Per definition wetting fluids have no entry-pressure whereas non-wetting fluids have, according to the definition of Young's Laplace equation (paragraph 2.4). Therefore, elemental mercury should be non-wetting since it has an entry-pressure, as reported by Devasena and Nambi, 2010. In a quartz system, water is wetting to air, air is wetting to mercury (with a contact angle of 130-140° according to MIP) and so water should be wetting to elemental mercury. The field-observations indicate mercury to be non-wetting, since it is present as blobs filling pores (fig. 16). If mercury was wetting, it would have been present in thin films instead of large blobs. This is illustrated in glass-beads experiments for water-air (or the equivalent PCE-air), where air accumulates in the pores and water or PCE in the pore throats, at lower water contents (Schwille *et al.*, 1988). However, at high PCE or water saturation, interconnected blobs and ganglia might become present and therefore inhibiting the distinction of wettability by pore body occupation. Nevertheless, the mercury blobs indicate it to be non-wetting in the saturated zone for sandy soils. At the other hand, elemental mercury can be the wetting phase in organic-rich soils, such as some types of loam or clay, which would result in slower migration of elemental mercury. For example, in figure 11, elemental mercury is still migrating after 100days, whereas non-wetting mercury becomes entrapped after 20 hours, in a hypothetical saturated homogeneous medium sand (paragraph 5.1.3). During this research elemental mercury is considered to be a non-wetting DNAPL and therefore is comparable to PCE in the saturated zone.

Assumptions made by modelling elemental mercury as a DNAPL in multi-phase-flow processes includes a continuous flow and the application of Leverett scaling. The first assumption is that elemental mercury flows in a continuous manner rather than in discontinuous spherical blobs. This is confirmed by the presence of a Pc(S) curve for water-mercury systems and applicability of van Genuchten-Mualem model on MIP data (Romero and Simms, 2008). The second assumption is the application of Leverett scaling, which enables modelling of different porous media by correcting the Pc(S) curve for different surface tensions, preventing large experimental efforts to be done. For regular DNAPLs this method applies reasonably on permeable soils (Busby *et al.*, 1995; Lenhard and Parker, 1987b). On basis of entry-pressure elemental mercury in the saturated zone is considered scalable (Devasena and Nambi, 2010). However, this is only the case when the correction factor used in the aforementioned article is incorrect, which is suggested by the authors. Leverett scaling of typical entry-pressures corresponds well with measured entry-pressures, when plotting entry-pressure as function of grain size (paragraph 2.4; fig. 3), hence supporting the applicability of Leverett-scaling. In summary, multi-phase-flow models assume elemental mercury to flow in a continuous manner and to be Leverett scalable. These assumptions seem to be valid, even though little supportive data is present.

6.1.2 Influence of density, viscosity and residual saturation

By establishing the importance of several distinctive parameters for elemental mercury in a multi-phase-flow an understanding is gained on the difference in behaviour between PCE and elemental mercury. Elemental mercury is known for its high density, surface tension and viscosity from which the density and surface tension are considered important according to the bond- and capillary number (Devasena and Nambi, 2010). The capillary pressure of elemental mercury is low, indicating a higher influence of capillary forces over viscous forces, compared to that of PCE. The bond number for elemental mercury is in the same order of magnitude as for PCE, indicating similar capillary forces to gravitational forces ratio for both DNAPLs. To determine the influence of density, viscosity and residual saturation on flow processes and final distribution of elemental mercury, sensitivity analyses were done.

The density of elemental mercury is the driving force for vertical migration, since it is 13.5 times higher than that of water and higher than that of PCE (13.500 kg m^{-3} and 1.650 kg m^{-3} for elemental mercury and PCE, respectively). Elemental mercury migrates faster than PCE in multiple model scenarios, for example scenarios with fine sand and a loam lens and fractured Crozier loam (*scenario C* and *scenario D*). This because the time required for reaching equilibrium is in *scenario C*: 25 and 30 hours and in *scenario D*: 30 and 35 hours, for elemental mercury and PCE, respectively. PCE was used to mimic elemental mercury migration in a saturated homogeneous medium sand (*scenario A*; paragraph 5.2.2; fig. 10), with an infiltration pressure of 90cm PCE head and a residual saturation of elemental mercury. The final distribution was similar to that of elemental mercury, however PCE required more time to reach equilibrium, due to the difference in density (20 and 35 hours for elemental mercury and PCE, respectively). Viscosity would hypothetically decrease flow velocity of elemental mercury more than that of PCE, however the influence of viscosity on elemental mercury migration is not significant, hence it would not alter the observation that PCE is slower than elemental mercury. Moreover, the importance of density on elemental mercury migration is illustrated when changing its density to that of PCE (paragraph 5.1.2; fig. 8B). The vertical infiltration characterizing mercury migration is gone, hence the major driving force is removed and the capillary and viscos forces become important. The time required to reach steady state has increased as well from 20 hours to 25 hours. In summary, the density of elemental mercury is the major force acting on its migration and is higher than the density of PCE, which results in a faster migration of elemental mercury than PCE. However this increase in velocity is not proportional to the difference in density, since parameters as viscosity influence migration as well.

Residual saturations for elemental mercury are low compared to that of PCE. In the vicinity of a chlor-alkali-plant, the residual saturation ranges from 0.05 to 0.30 for sandy soils. Whereas measured values in a short-column experiment were 0.08 and 0.04 for medium and coarse sand (Devasena and Nambi, 2010). Consequently, the model shows low residual saturations from which 0.01 is set as minimum, otherwise numerical dispersion might become too large within the results. PCE has residual saturations of 0.168 and 0.275 for coarse and medium sand, respectively, whereas in another study it is 0.120 and 0.126 for coarse and fine sand, respectively (Devasena and Nambi, 2010; Hofstee *et al*., 1998). The lower residual saturation for elemental mercury compared to PCE in the same soil is most likely due to the high density and high surface tension of elemental mercury. Since the high

density of elemental mercury inhibits accumulation and the high surface tension inhibits surface formation, hence it tends to remain in a continuous flow with lower surface areas. The difference between residual PCE and mercury on micro-scale is illustrated in photos taken in the vicinity of a chlor-alkali-plant. Where PCE tends to randomly form ganglia around peninsulas of water and result in residual saturations (Schwille *et al.*, 1988), mercury forms distinctive non-spherical blobs in different shapes. This might be a consequence of the high surface tension of mercury. An assumption taken by comparing glass-beads experiments by Schwille *et al*., 1988 and in-situ mercury photos is the difference between large glass-beats and sand grains. The effect of the difference in residual saturation on reconnecting blobs, during a later-stage flow of mercury through the same soil, is not known and might differ from PCE. So, elemental mercury exhibits lower residual saturations than PCE and forms blobs rather than random ganglia.

As a consequence of the low residual saturation of elemental mercury in porous media, mercury tends to migrate further than PCE. During this research, modelling of both mercury and PCE indicated mercury to migrate further with the same volume, even though the boundary condition for PCE decreased the infiltration depth due to an artificial horizontal spreading at the top. For example, when 1.5m³ of mercury infiltrates in a perfectly homogeneous porous media to 32 meters, the same volume of PCE does 11 meter (paragraph 5.1.1; *scenario A*), adding heterogeneities yields the same tendency (*scenario C* and *scenario D, paragraph: 5.2.1 and 5.2.2*). Field observations indicate a large penetration depth of elemental mercury in the subsurface. In the vicinity of a chlor-alkali-plant elemental mercury was found at depths of 9m, with rather low residual saturations. In Onogada lake, New York, elemental mercury was found at depths of 16.8meters. Elemental mercury tends to infiltrate deeper than PCE for the same spill characteristics (e.g. NAPL volume, surface area of contamination, continuous or discontinuous flux and time framework). This does not imply elemental mercury infiltrates deeper than PCE, since more PCE might have spilled and therefore resulting in a deeper infiltration.

So, elemental mercury migration is governed by its high density, which is exceptionally high compared to that of PCE and water. The viscosity of elemental mercury slightly inhibits flow, but is not significant during mercury migration since the density is significantly higher. Whereas the residual saturation is low for elemental mercury, enabling elemental mercury to migrate further than PCE for the same contamination history and characteristics.

6.1.3 Influence of preferential flow on elemental mercury

In natural occurring soils heterogeneities are common and hence influencing NAPL flow. Therefore the influence of heterogeneities on mercury migration is investigated and compared to that of PCE. The hypothesis is that flow of elemental mercury will commence via preferential pathways (i.e. low entry-pressure, high hydraulic conductivity etc.). Since elemental mercury has a high tendency to continue migration due to its high density and therefore it might be an energetic favourable option. In the case of a loam lens within saturated fine sand, mercury will tend to flow over the lens rather than infiltrating loam, which is comparable to the behaviour of PCE (*scenario C*; fig. 12), where PCE requires 5 times the volume of elemental mercury and requires more time to reach steady-state. In the case of an intact loam layer in a fine sand aquifer, both elemental mercury and PCE will

infiltrate after a short period of horizontal spreading at the interface of loam and fine sand (*scenario D*; fig. 13A and 13C). Elemental mercury flows vertically until flow ceases due to the loam layer, consequently it will flow horizontally in a rather flat layer with almost a perpendicular flow direction, whereas PCE tends to accumulate on top of the loam layer, rather than spreading horizontally. Accumulation of elemental mercury in height is an unstable situation, due to its exceptionally high density, hence it tends to flow either vertical or horizontally to obtain a most energetic favourable situation. A fractured zone in the loam layer results in a preferential flow and inhibits both mercury and PCE infiltration in to the loam. In this manner, PCE and elemental mercury are rather similar in behaviour within heterogeneities. The large horizontal spreading at a rather impermeable layer for elemental mercury might enhance flow via preferential pathways, since elemental mercury can continue horizontal spreading until it finds a fracture or other pathway. This is in contrast to PCE, which can simply accumulate in height on top of a rather impermeable layer. Consequently, this can explain the field-observation in the vicinity of a chlor-alkali-plant, which is that visible mercury seems to be present in sandy soils rather than impermeable soils. So, untraceable mercury might be present in finer-grained materials, a preferential flow may inhibit mercury infiltration in semi-impermeable layers or the residual saturation of low permeability layers is simply lower.

Elemental mercury and PCE have the ability to infiltrate semi-impermeable layers (e.g. loam, silt, clay). Assuming Leverett-scaling to apply on both DNAPLs, the entry-pressure of a DNAPL into a soil is subjected to ratio of density and interfacial tension. This ratio is the same for both DNAPLs, whereas the bond-number is in the same order of magnitude (paragraph 2.4). Consequently, the same entry-head is needed for PCE and elemental mercury in the same soil type, measured in its own entry-head (cm of PCE or cm of elemental mercury, respectively). For example, if PCE does not infiltrate clay then elemental mercury would not infiltrate clay as well, assuming equal NAPL-head. In this manner, elemental mercury and PCE have the similar behaviour of infiltrating heterogeneities.

In summary, both elemental mercury and PCE flow via preferential pathways rather than infiltrating semi-permeable soils (e.g. loam). Both DNAPLs have the same ratio between density and interfacial tension, hence the same behaviour of infiltrating a semi-impermeable layer or not. However, elemental mercury has a higher tendency to sustain flow in horizontal direction on top of a semi-impermeable layer, whereas PCE might accumulate easier on top of such an interface rather than flowing horizontally.

6.2 Elemental mercury in the unsaturated zone

The behaviour of elemental mercury is deviating from that of PCE in the unsaturated zone. PCE is the non-wetting phase in the saturated zone whereas in dry soil it is the wetting phase (Cohen and Mercer, 1990). In contrast, mercury is the non-wetting phase in both saturated and dry soil and therefore is used for porosimetry (MIP). In the unsaturated zone, during three-phase-flow between water, air and NAPL, PCE is considered to be intermediate wetting and non-spreading on a water-wet porous media (Hofstee *et al*., 1998). Elemental mercury is non wetting to air and therefore should be non-wetting in a three-phase-flow with a water-wet porous media. However the viscosity of air is significantly lower than that of mercury; hence it might be an unstable interface. Since, the wetting sequence of mercury in a three-phase-flow is not known it is assumed to be a non-spreading intermediate wetting DNAPL. Unfortunately, STOMP-WO version 1 does not include the spreading behaviour of DNAPLs and models all NAPLs as spreading fluids, implying an infinitely thin mercury layer as a consequence of the infinite spreading (Hofstee *et al*., 1998; Oostrom *et al*., 2003). So, on basis of wetting sequence elemental mercury differs from PCE in the unsaturated zone. How this is found in natural soils is not known and therefore requires fundamental research on wettability phenomenon.

Inherent to the unsaturated zone is the entry-pressure needed for DNAPL infiltration into the subsurface, which should be Leverett scalable to enable multi-phase-flow modelling. During MIP, Youngs Laplace equation is used to determine the entry pressure as a function of pore throat radii, this would be equivalent to Leveretts equation for entry-pressure. Since this scaling method is based on Leveretts equation correlating entry-pressure to pore radii, Leverett scaling seems to be applicable. In the research conducted by Aung *et al*., 2001, the retention curve for MIP was compared to that of the entry-pressure for water-air for clayey silt. By taking the ratio of the two entry pressures, 0.250 and 0.100 MPa, a factor of 0.6 could be determined, whereas taking the ratio of interfacial tensions a factor of 0.14 was determined (MIP: 485 dynes cm^{-1} and for water-air: 72 dynes cm^{-1}). It is known that less-permeable layers are not Leverett scalable, hence explaining the difference in ratio in clayey silt. Moreover, there is no research done on mercury in a multi-phase-flow in the unsaturated zone. Leveretts scaling seems to be applicable to mercury in dry-soils, by assuming the curvature of the interface between mercury and air or water to be the same within a soil. Based on Leverett scaling the entry pressure for mercury in dry medium and coarse sand would be 2.71 cm and 1.77 cm, whereas for saturated medium and coarse sand it is 2.15 cm and 1.37 cm, respectively. This is a minor difference for medium and coarse sand, but at less-permeable layers with higher entry-pressures the factor might become of importance. Entry-pressures at the surface can be overcome by a small mercury accumulation where its head becomes higher than the entry pressure, for example: pool formation, preferential flow in small fractures, leakage from a tube in the soil, flow via roots and so on. However, the entry-pressure as a function of water saturation in the unsaturated zone is not yet fully understood and might strongly influence mercury infiltration in the unsaturated zone. A final remark: it is assumed that chemical- and physical processes such as adsorption and temperature differences, do not decrease the surface tension of mercury. However, it is reported that water adsorption decreases the surface tension quite extensively, whereas other adsorption processes like oxidation are not significant (Wilkinson, 1972). In summary, elemental mercury needs an entry-pressure for dry soil in

contrast to PCE and therefore differs from PCE in an unsaturated zone, which consequently would affect distribution of elemental mercury in the saturated zone.

Models on elemental mercury in the unsaturated zone indicate mercury to behave different than PCE (paragraph 5.3; *scenario E*). Heterogeneities in the unsaturated zone seem to be impermeable for elemental mercury to infiltrate (fig. 14B). In this case, mercury tends to spread horizontally at the lithology interface between coarse- and fine sand. After interference with the boundary condition, a pressure head builds up and allows infiltration. Whilst, PCE penetrates the fine-sand heterogeneity easily, indicating the interfacial tension of mercury to be too high compared to its NAPL pressure at 10cm depth. Hofstee *et al*., 1998, established the difference of spreading vs. non-spreading of PCE, by comparing experimental results with model results. It seems that models were able to predict the initial behaviour of PCE but not the final distribution. Therefore, modelling mercury as a spreading-liquid is thought to be representative for the process during flow and not for determining final distributions. Hence, the lack of infiltration by mercury in unsaturated fine sand seems reasonable. Even though, the horizontal spreading obtained in this research for elemental mercury (fig. 14B) is a consequence of the assumption of a spreading-liquid. It seems that heterogeneities in the unsaturated zone influences mercury migration, since the entry-pressure of less-permeable layers is too high.

In the unsaturated zone mercury vapour acts as another pathway for mercury migration, due to the vaporization and condensation of mercury vapour. Low residual saturations for mercury, 10^{-7} to 10^{-8}, are a result of migration via the vapour-phase (appendix E). This process was observed for PCE in glass-beats experiments (Schwille *et al*., 1998). Consequently, low residual saturations in the unsaturated zone imply transport via vapour rather than the liquid phase and should not be confused with each other.

Finally, elemental mercury shows a slightly different behaviour at the water table than PCE. When a PCE plume enters the saturated zone it horizontally increases in size, whilst mercury horizontally decreases in size (fig. 10). This might be the result of the lower interfacial tension for mercury in water than air. This is in contrast to PCE, hence interfacial tension for PCE is higher in water than air. For PCE, Pc(s) curves are lower in air than water. Therefore a pressure head is needed to account for this difference, hence the horizontal spreading at either the water table or the capillary fringe. In summary, PCE spreads horizontally at the capillary fringe whereas mercury horizontally decreases its size.

The behaviour of elemental mercury differs in the unsaturated zone from PCE. Both DNAPLs are non-spreading, but elemental mercury is non-wetting to air whereas PCE is wetting to air. Assumptions made on Leverett-scaling and continuous flow seems applicable on MIP and therefore also on multi-phase-flow models, in general. By assuming a spreading DNAPL, mercury does not infiltrate a fine sand heterogeneity, whereas PCE does. Nevertheless, experimental results are needed to thoroughly understand and calibrate multi-phase-flow models for the unsaturated zone.

6.4 Implications of this study

The implications of this study on elemental mercury remediation and assessments is given in this paragraph. The behaviour of elemental mercury in soil is such that contamination by its liquid phase is problematic and requires different remediation strategies; especially at larger depths. As indicated by the results on mercury migration in the saturated zone, it tends to infiltrate deep and leaves a low residual saturation. Contaminations at depths of 16.8 meters are extremely complicated to remove, such that it acts as a source for mobile mercury species over long periods. After years of spilling an unknown volume, it can have penetrated to extensive depths and over several horizontal interfaces. It might infiltrate through a loam layer or preferentially via either fractured zones or other heterogeneities, indicating it will continue to migrate downwards. Add to this the high toxicity of mercury in any form, for both humans and ecosystems, it makes a mercury pollution extremely hazardous and persistent.

In order to establish models on the mercury distribution and possible remediation methods at a contamination sites, a thorough understanding is needed on the flow behaviour in different soils. Since the groundwater condition in which residual mercury is located is important to determine, in order to evaluate the risk of mobile, and more dangerous, mercury species. After recognition, mobile mercury species can be remediated by, for example, using the process of adsorption of mercury on sulphur, activated carbon or silica-capsules. Elemental mercury vapour is a mercury species to keep track of in the unsaturated zone, since it might accumulate and become a risk in basements. Finally, processes in the unsaturated zone need to be investigated, since it might prevent mercury from infiltrating the subsurface. So a thorough understanding of elemental mercury migration through the subsurface is needed to evaluate the location of residual mercury and the risk on mobile mercury species.

Elemental mercury in the subsurface is a contaminant of concern. Where recent developments are increasing knowledge on the behaviour of mercury in porous media, this study focusses on elemental mercury in its liquid form. In general, contaminations close to the surface can be remediated by stripping mercury vapour from the unsaturated zone, heating soil and old-fashioned excavation. Research questions on mercury in the unsaturated zone are abundant, since it is not comparable to any regular DNAPL. However, deeper in the subsurface (i.e. the saturated zone) mercury seems to behave rather similar to PCE, but then more mobile and migrating faster. Unfortunately, elemental mercury tends to penetrate exceptionally deep, if it penetrates the subsurface, which would result in persistent contaminations. Current knowledge on DNAPL remediation in deep aquifers has to be evaluated on its applicability on elemental mercury. Since viscous forces are considered not important to elemental mercury, pump and threat methods based on increasing capillary number might not be successful. So, knowledge on the behaviour of elemental mercury in the subsurface is not yet sufficient to determine possible remediation strategies for large depths.

6.5 Recommendations

In this section recommendations on the study of elemental mercury in the subsurface are made to indicate the lack of understanding on its behaviour. In general, experiments have to be conducted to confirm multi-phase-flow models, such as STOMP, since elemental mercury is not a regular DNAPL (e.g. PCE). This to establish models of higher quality, due to more accurate parameters determined in experiments.

Firstly, the chemical interactions between groundwater and elemental mercury need to be determined to establish the true potential of residual mercury to contaminate groundwater. PCE is an organic solvent, whereas elemental mercury is a metallic liquid, this would yield differences in chemical interactions, adsorption processes and biological processes. Elemental mercury is a strong reducing compound and therefore its chemistry in groundwater might differ and hence need to be investigated further.

In the unsaturated zone the fundamentals of mercury migration are not understood and therefore require experimental research. These fundamentals include spreading processes on the water-air interface and the wetting sequence of mercury. In this case micro-bead experiments would be useful, in order to obtain an insight into micro-scale processes of wettability and spreading-phenomena, for example the research conducted by Schwille *et al.*, 1988. The entry-pressures for different lithologies in the unsaturated zone are needed, this to establish whether mercury would infiltrate the subsurface or not, hence governing infiltration of mercury in the subsurface. Mercury is non-wetting in dry-soils whereas PCE is wetting, consequently it might influence Pc(S) curves in the unsaturated zone. Hence, research on the Pc(S) curve for three-phase-flow between air, mercury and water is needed (i.e. is Leverett-scaling applicable or not). In summary, the behaviour of elemental mercury in the unsaturated zone is not fully understood, due to the lack of experimental data.

In general, the applicability of current multi-phase-flow models for regular DNAPLs on elemental mercury needs to be validated. For the saturated zone the low-residual saturation and the large penetration depth of mercury have to be experimentally investigated, since the residual saturation dictates its final distribution. Basically, the results of this research on multi-phase-flow models require experimentally proof and explanations. This would allow modelling of field-scale scenarios. By using micro-scale bead experiments and column experiments in the laboratory, processes indicated in this report can be investigated. This would enhance understanding on mercury migration and possibilities on remediation by surfactants, pump and threat, stripping and other procedures.

Chapter 7: Conclusion

Elemental mercury is a non-wetting DNAPL in the saturated zone, therefore comparable to the better known PCE. This enables multi-phase-flow modelling of elemental mercury in the saturated and possible the unsaturated zone, by assuming Leverett scaling and continuity of flow to be valid. The results on saturated homogeneous porous media indicate that flow of elemental mercury is governed by its exceptionally high density, whereas the influence of its high viscosity is limited. As a consequence of its low residual saturation and high density, elemental mercury is able to infiltrate further in soils than PCE, at the same volume of DNAPL spill. In saturated heterogeneous porous media, both elemental mercury and PCE flow via preferential pathways. The ability of both DNAPLs to infiltrate less-permeable layers is similar, since the ratio between density and interfacial tension is the same, assuming Leverett-scaling to apply on elemental mercury. However, elemental mercury does migrate faster and further than PCE in soil and groundwater systems. In the unsaturated zone the behaviour of elemental mercury seems also to deviate from that of PCE, since mercury is non-wetting to air whereas PCE is wetting to air. Even, when assuming both DNAPLs to be intermediate wetting, PCE is able to infiltrate fine sand whereas elemental mercury is not. This implies heterogeneities in the unsaturated zone to inhibit mercury migration, whereas in the saturated zone mercury seems to maintain flow in heterogeneous porous media. Further experimental research is required to validate current two-phase-flow models on elemental mercury in the saturated zone and to establish fundamental multi-phase-flow processes in the unsaturated zone. This would enable models to simulate mercury contaminations and allow development of new or re-applied remediation methods.

Acknowledgments

I would like to thank several people who have contributed to this research and without whom I wouldn't have been able to produce such a report. Firstly, I would like to thank Prof. Dr. Majid Hassanizadeh for pointing out this project to me and for helping me with difficult questions on multi-phase-flow. I would like to thank Dr. Niels Hartog for the unlimited supply of ideas for answering the research questions. Special thanks goes to Dr. Annemieke Marsman, without whom modelling software STOMP and its according multi-phase-flow theorem would have been too complicated to get it to work. I would also like to thank Dr. Thomas Keijzer for the practical insight into mercury contaminations and knowledge on real mercury contaminations. Finally, I would like to thank Dr. Cor Hofstee for his comments on mercury in the unsaturated zone and its wettability phenomena.

References

Aung K.K., Rahardjo H., Leong E.C., Toll D.G., 2001. Relationship between porosimetry measurement and soil-water characteristic curve for an unsaturated residual soil. Geotechnical & Geological Engineering 2001, Volume 19, Issue 3-4 pp 401-416

Busby R.D., Lenhard R.J., Rolston D.E., 1995. An Investigation of Saturation-Capillary Pressure Relations in Tow-and-Three-Fluid Systems for Several NAPLS in Different Porous Media. Vol. 33, No. 4- Groundwater-July-August 1995.

Cohen M. C., Mercer J.M., 1990. A review of immiscible fluids in the subsurface: Properties, models, characterization and remediation. Journal of Contaminant Hydrogeology 6 (1990) 107-163.

Devasena M., Nambi I. M., 2010. Migration and entrapment of mercury in porous media. Journal of Contaminant Hydrology 117 (2010) 60-70

Diamond S., 2000. Mercury porosimetry: An inappropriate method for the measurement of pore size distributions in cement-based materials. Cement and Concrete Research, Volume 30, Issue 10, October 2000, Pages 1517-1525.

Eichholz, G. G., Petelka M. F., Kury R. L., 1986. Migration of elemental mercury through soil from simulated burial sites. Wat. Res. Vol. 22, No 1, pp. 1520, 18.

EuroChlor: http://www.eurochlor.org/chlorine-industry-issues/mercury.aspx, visited at 3-february-2013.

Deeb R., Hawley E., Kell L., O'Laskey R., 2011. Assessing Alternative Endpoint for Groundwater Remediation at Contaminated Sites. ESTCP Project.

Deltares: http://www.deltares.nl/nl/actueel/nieuwsbericht/item/11429/camerasonde-levert-waardevolle-informatie-op?highlight=kwik , visited 15-february-2013.

Ellison A. H., Klemm R. B., Schwartz A. M., 1967. Contact Angles of Mercury on Various Surfaces and the Effect of Temperature. Journal of Chemical and Engineering data, vol. 12, No. 4, October 1967.

Fetter C.W.,1999. Contaminant hydrogeology. Waveland Press, Inc. pp.208-263.

French H.K., van der Zee S.E.A.T.M., Leijnse A., 2000. Prediction uncertainty of plume characteristics derived froma a small number of measuring points. Hydrogeology Journal (2000) 8: 188-199

Gabriel M. C., Williamson D. G., 2004. Principal biogeochemical factors affecting the speciation and transport of mercury through the terrestrial environment. Environmental Geochemistry and Health 26: 421-434. 2004.

Genuchten M. Th. van. A Closed-form Equation for Predicting the Hydraulic Conductivity of Unsaturated Soils. Soil Science Society of America Journal Vol. 44, no. 5, September-October 1980.

Good R. J., 1981. The contact angle in Mercury Intrusion Porosimetry. Powder Technology, 29(1981) 53-62.

Massacci P., Piga L., Ferrini M., 2000. Application of physical and thermal treatment for the removal of mercury from contaminated materials. Minerals Engineering, 13(2000), Isues 8-9, pp. 963-967

Hofstee C., Oostrom M., Dane J. H., Walker R. C., 1998. Infiltration and redistribution of perchloroethylene in partially saturated stratified porous media. Journal of Contaminant Hydrology 34 (1998) 293-313.

Horvat M., Nolde N., Fajon V., Jereb V., Logar M., Lojen S., Jacimovic R., Falnoga I., Liya Q., Faganeli J., Drobne D., 2002. Total mercury, methyl mercury and selenium in mercury polluted areas in the province Guizhou, China. The Science of the Total Environment 304 (2003) 231-256

Ippisch O., Vogel H. J., Bastian P., 2006. Validiy limits for the van Genuchten-Mualem model and implications for parameter estimation and numerical simulation. Advances in Water Resources 29-12 (2006) 1780-1789.

ITRC, 2012. Using Remediation Risk Management to Address Groundwater Cleanup Challenges at Complex Sites. Page 31.

Kueper B.H., Frind E.O., 1991. Two-Phase Flow in Heterogeneous Porous Media 2. Model Application. WATER RESOURCES RESEARCH, VOL. 27, NO. 6, PAGES 1059-1070, JUNE1991.

Kloubek J., 1981. Hysteresis in porosimetry. Powder Technology 29-1(1981) 63-73

Lenhard R.J., 1994. Scaling Fluid Content-Pressure Relations of Different Fluid Systems in Porous Media. Hydrology Days Conference April 5-9, 1994.

Lenhard R.J., Parker J.C., 1987a. A Model for Hysteric Constitutive Relations Governing Multiphase Flow 2. Permeability-Saturation Relations. Water Resource Research, VOL. 23, NO. 12, PAGES 2197-2206, December 1987.

Lenhard R.J. and Parker J.C., 1987b. Measurement and Prediction of Saturation-Pressure Relationships in Three-Phase Porous Media Systems. Journal of Contaminant Hydrology, 1(1987) 407-424.

Leverett M.C., 1941. Capillary behaviour in porous solids. American Institute of Mining and Metallurgical Engineers Transactions, Petroleum Development and Technology 142, 152-169.

Matthews G.P., Ridgway C. J., Spearing M. C., 1995. Void space modeling of Mercury intrusion hysteresis in Sandstone, Paper Coating and other Porous Media. Journal of Colloid and Interface science 171, 8-27 (1995).

Mayer A., Hassanizadeh S. M., 2005. Soil and Groundwater Contamination: Non Aqueous Phase Liquids. American Geophysics Union books board.

EPA, 2003. Federal Register. Vol. 68, No. 244: http://www.gpo.gov/fdsys/pkg/FR-2003-12-19/pdf/03-22926.pdf

Parker J.C., Lenhard R.J., 1987. A Model for Hysteric Constitutive Relations Governing Multiphase Flow 1. Saturation-Pressure Relations. Water Resource Research, VOL. 23, NO. 12, PAGES 2187-2196, December 1987.

Pau G., Fuchs F., Skylar O., Boutros M., Huber W., 2010. EBImage-an Rpackage for image processing with applications to cellular phenotypes. Bioinformatics (2010) 26(7): 979-981.

Pau G., Skylar O., Huber W., 2012. Introduction to EBImage, an image processing and analysis toolkit for R.

Rigby S. P., Edler K. J., 2002. The Influence of mercury Contact Angle, Surface Tension, and Retraction Mechanism on the Interpretation of Mercury Porosimetry Data. Journal of Colloid and Interface Science 250, 175-190 (2002).

RIVM: www.RIVM.nl: Kwik en Kwik verbindingen: visited at 3-februari-2013.

Romero E., Simms P. H. (2008). Microstructure Investigation in Unsaturated Soils: A Review with Special Attention to Contribution of Mercury Intrusion Porosimetry and Environmental Scanning Electron Microscopy. Geotech Geol Eng (2008) 26: 705-727.

Salmas C., Androutsopoulos G., 2001. Mercury porosimetry: Contact Angle Hysteresis of Materials with Controlled Pore Structure. Journal of Colloid and Interface Science 239, 178-189 (2001).

Šimůnek J., Jarvis N. J., Genuchten M. Th. Van., Gärdenäs A., 2003. Review and comparison of models for describing non-equilibrium and preferential flow and transport in the vadose zone. Journal of Hydrology 272:1-4 (2003) 14-15

Scanlon B.R., Tachovsky J.A., Reedy R., Nicot J.P., Keese K., Slade R.M., Merwad V., Howard M.T., Wells G.L., Mullins G.J., Ortiz D.M., 2005. Groundwater-Surface Water Interactions in Texas. Bureau of Economic Geology, page: 129-131.

Schuster E., 1991. The behaviour of mercury in the soil with special emphasis on complexation and adsorption processes- a review of the literature. Water, Air and Soil Pollution 56: 667-680, 1991.

Schwille, F., 1988. Dense Chlorinated Solvents in Porous and Fractured Media Model Experiments. Lewis Publishers, Chelsia, MI.

Spitzer Z., (1981). Mercury Porosimetry and its Application to the Analysis of Coal Pore Structure. Powder Technology, 29 (1981) 177-186

Taube F., Pommer L., Larsson T., Shchukarev A., Nordin A., 2008. Soil Remediation- Mercury Speciation in Soil and Vapor Phase During Thermal Treatment,. Water, Air and Soil Pollution, 193 (2008), Issue 1-4, pp. 155-163.

Walvoord M. A., Andraski B. J., Krabbenhoft D. P., Striegel R. G., 2008. Transport of elemental mercury in the unsaturated zone from a waste disposal site in an arid region. Applied Geochemistry 23 (2008) 572-583

Wang J., Feng X., Anderson C.W.N., Xing Y., Shang L., 2012. Remediation of mercury contaminated sites – A review. Journal of Hazardous Materials 221-222 (2012) 1-18

Wardlaw N. C., McKellar M., 1981. Mercury Porosimetry and the interpretation of Pore geometry in Sedimentary Rocks and Artificial Models. Powder Technology, 29 (1981) 127-143.

Wilkinson M. C., 1972. The surface properties of mercury. Chemical Reviews, VOL 72 -6, 1972

White M.D., Oostrom M., 2000. STOMP Subsurface Transport Over Multiple Phases- Theory guide.

Appendix

The behaviour of elemental mercury in porous media

T. Sweijen

Appendix A: Contact angle mercury in a water-mercury-quartz system

The contact angle for mercury-water on quartz is not readily known, therefore a small calculation is done by using a line tension balance and typical data for elemental mercury (Fig. 1 and Table A1). First, the unknown interfacial tension between quartz and mercury is determined by using a mercury-air-quartz system, then the contact angle for elemental mercury in a mercury-water-quartz system is solved.

	Interfacial tension [dynes cm]	*Reference*
σ_{wa}	72	Mayer and Hassanizadeh, 2005
σ_{wm}	375	Wilkinson, 1972
σ_{ma}	485	Wilkinson, 1972
σ_{sa} (quartz)	43	Bachmann *et al.*, 2007
θ_{ma}	130	Wilkinson, 1972

Table A1: Typical interfacial tensions needed to determine the contact angle between mercury and water in respect to quartz.

First, the interfacial tension between elemental mercury and quartz is determined by using a better known air-mercury quartz system. The following equation describes the line tension balance in such a system:

$$cos\ \theta_{ma} = \frac{\sigma_{sa} - \sigma_{ms}}{\sigma_{ma}}$$

Which can be rewritten and solved to:

$$\sigma_{ms} = \sigma_{sa} - \sigma_{ma} \cos\theta_{ma} = 43 - 485 \cos 130 = \ 354.8\ dynes\ cm^{-1} \quad \text{(eq. A2)}$$

Next, an estimation of the interfacial tension between water and quartz is done by using Antonow's rule, equation A3 (Kwok and Neumann, 2000).

$$\sigma_{sw} = |\sigma_{wa} - \sigma_{sa}|$$

Which can be solved to:

$$\sigma_{sw} = 72 - 43 = 29\ dynes\ cm^{-1}$$

Finally, the contact angle of mercury can be calculated by using

$$\cos\theta_{mw} = \frac{\sigma_{sw} - \sigma_{ms}}{\sigma_{wm}} \qquad \theta_{mw} = 150.3°$$

This results in a contact angle of θ_{mw}=150.3°, confirming the non-wettability of mercury in a water-mercury-quartz system

Appendix B: Centre of mass and Variance

During this research spatial moments were used to determine the plume shape, to allow comparison between multiple results. The graphs are ordered according to the order of results, first saturated homogeneous porous media, then heterogeneous porous media and finally the unsaturated zone. In each graph the depth of the center of mass is given on the left-hand y-axis and the horizontal variance at the right-hand Y-axis.

B.1 Homogeneous saturated porous media

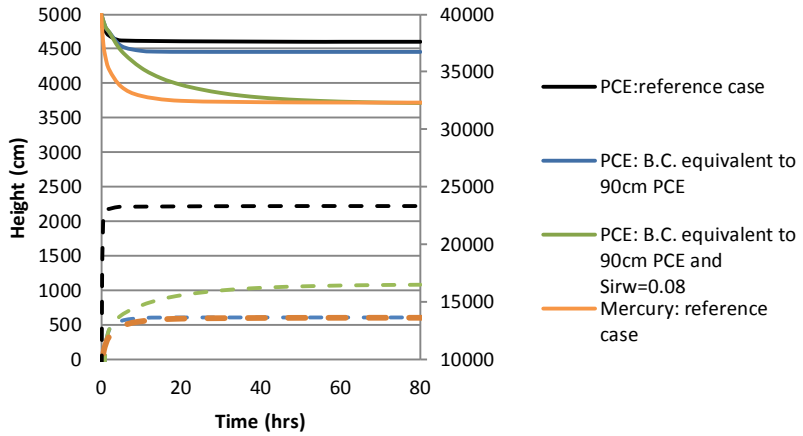

Fig. B1: PCE and mercury spill in a saturated medium sand, to illustrate the influence of several boundary conditions. With original PCE and mercury spills as reference case and two graphs describing influence of an infiltration-pressure equivalent to 90cm of PCE instead of 90cm of mercury head and the influence of low-residual saturation.

B.2 Heterogeneous saturated porous media

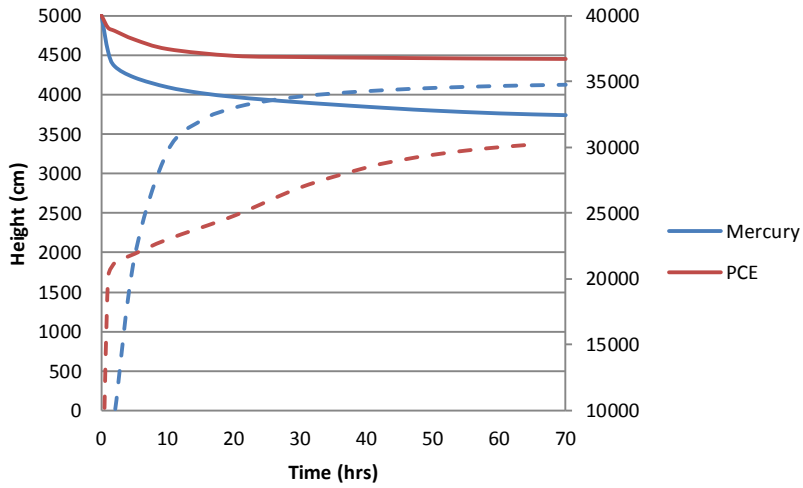

Fig. B2: Mercury and PCE leakage in heterogeneous saturated fine sand, with a loam lens. The sudden gradient changes are due to the presence of a loam layer.

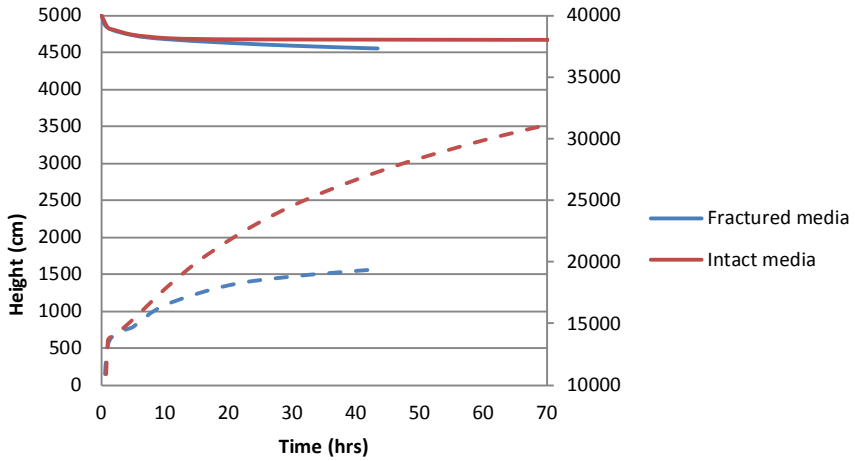

Fig. B3: PCE leakage in heterogeneous saturated fine sand, with a('fractured') loam layer.

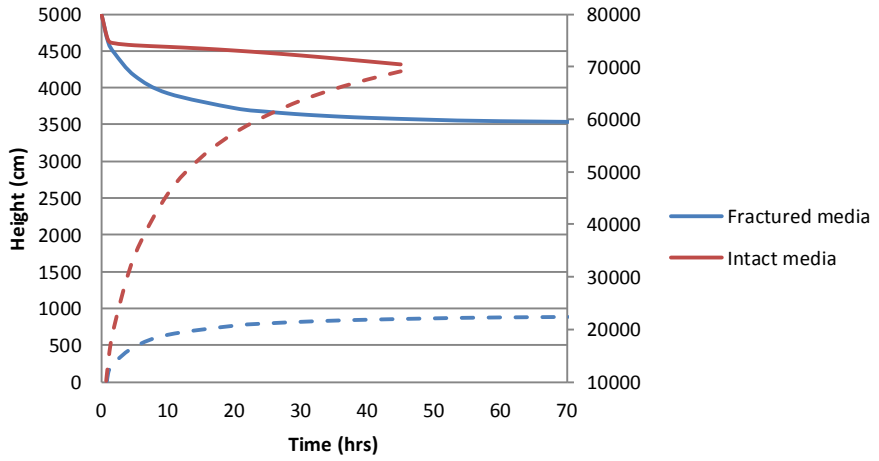

Fig. B4: Mercury leakage in heterogeneous saturated fine sand, with a('fractured') loam layer.

B.3 Three-phase-flow

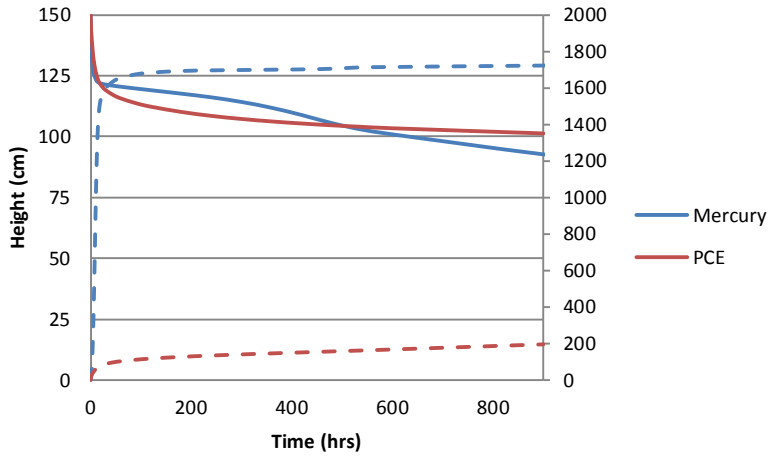

Fig. B5: Mercury and PCE leakage in a heterogeneous unsaturated porous media, according to Hofstee et al., 1998. Variance for PCE is significant lower than for elemental mercury.

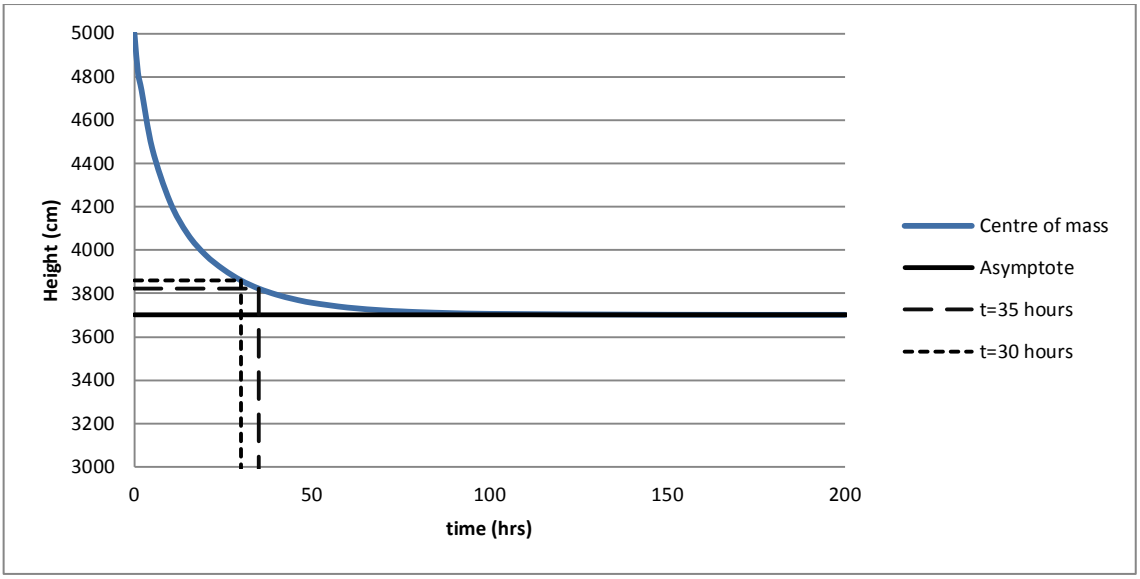

Fig. B6: this figure shows the asymptote, definition of time of entrapment and a non-specified center of mass graph. The change in center of mass within 5 hours is less than 1% between 30 hours and 35 hours.

Appendix C: Additional model results

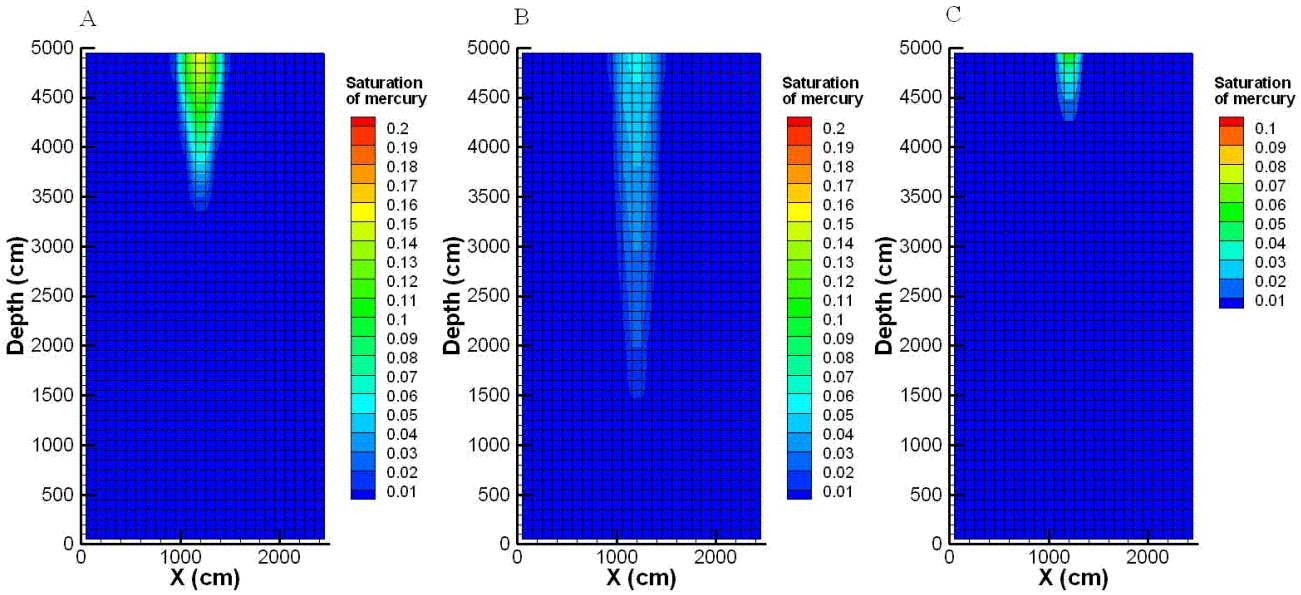

Fig. C1: DNAPL leakage in a saturated zone, consisting of medium sand, for illustrating different boundary conditions. A) Boundary condition is equivalent to 90cm head of PCE instead of 90cm equivalent head of mercury, with 1.5m³ PCE. B) Boundary condition is equivalent to 90cm head of PCE instead of 90cm equivalent head of mercury and a residual saturation equal to that of mercury in the saturated zone, with 1.5m³ PCE. C) Elemental mercury with an equal mass to that of PCE, 2450 kg or 0.18 m³, with normal boundary conditions.

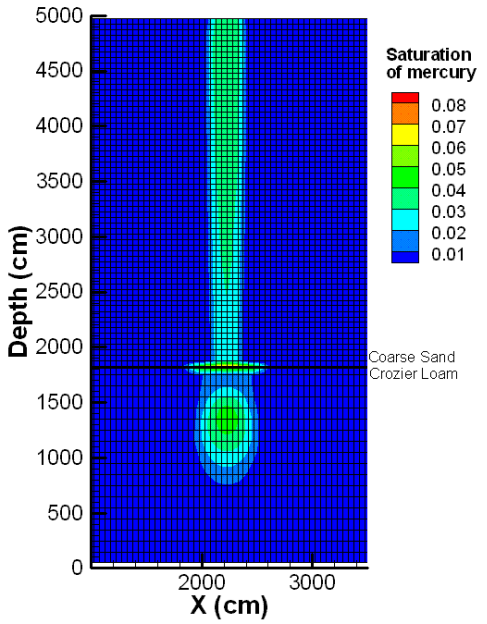

Fig. C2: Elemental mercury leakage in a saturated zone consisting of Crozier Loam with coarse sand on top. The artificial looking result indicates infiltration of elemental mercury in the loam at high enough NAPL pressure.

Appendix D: Mercury Intrusion Porosimetry (MIP)

Mercury Intrusion Porosimetry (MIP) is used for determination of pore size distribution in porous media. This method is based upon the principle that mercury is non-wetting in respect to air and therefore needs an external pressure to overcome certain entry pressures (Rigby and Edler, 2002; Romero and Simms 2007). Therefore it is considered to be a two-phase flow between air and mercury, which has been extensively investigated.

For doing the MIP experiment, a sediment sample is dried and put into vacuum, next they are put into a container with elemental mercury. Then, pressure is applied at the mercury reservoir, such that an entry pressure is overcome and the volume of the mercury will change. This is done stepwise and will result in incremental volume-pressure changes, which can be converted to radius-volume graph by using the Washburn equation (Romero and Simms, 2007; Diamond, 2000).

$$P = -\frac{2\gamma \cos\theta}{r}$$

γ = surface tension
θ = contact angle
r = the radius
P = entry pressure

In order to get a duplicate, the measurement is done during drainage and imbibition, resulting in entrapment of mercury. Since the common use of this method, the quality and drawback of the method has been extensively evaluated, from pore network modeling to large-scale porous media properties.

First, the hysteresis between drainage and imbibition of mercury is considered. For hysteresis a range of porous media properties appears to be important: pore size distribution, ratio between pore and throat sizes, heterogeneities and surface roughness (Matthews *et al*., 1995; Wardlaw and McKellar, 1981). In the case of pore size distribution, more entrapment will occur with a wide pore size distribution than with a narrow pore size distribution, hence inducing hysteresis (Rigby and Edler, 2002; Wardlaw and McKellar, 1981). This is induced by the presence of heterogeneities, for example: when a group of macroscopic pores is surrounded by microscopic pores, mercury entrapment will occur (Rigby *et al*., 2003). Moreover, it appears that during drainage, mercury preferentially fills larger pores before smaller pores and during imbibition mercury evacuates first from smaller pores then larger pores. By the time the pressure dropped in larger pores to the entry pressure of mercury, snap-off has already occurred, inducing mercury entrapment (Wardlaw and McKellar, 1981; Rigby and Edler, 2002; Ioannidis *et al*., 1990). This phenomenon will happen in a wide pore size distribution, rather than a narrow pore size distribution. Next, a wide range of pore size distribution will induce a larger difference between pore sizes and throats, which induces snap-off as well (Rigby and Edler, 2002; Matthews and McKellar, 1981). Finally, the contact angle of mercury with air is dependent on the surface roughness, which might result in more contact angle hysteresis during imbibition (Matthews *et al.*, 1995; Good, 1981). The contact angles used in Mercury Intrusion Porosimetry is given in table D1.

In order to correct for hysteresis between drainage and imbibition, due to porous media properties described above, an empirical relation has been determined for drainage and imbibition, equation C2 and C3, respectively (Rigby and Edler, 2002).

$$\gamma cos\theta_A = -302.533 + \frac{-0.739}{r} \qquad \text{(Equation. D2)}$$

$$\gamma cos\theta_R = -68.366 + \frac{-235.561}{r} \qquad \text{(Equation. D3)}$$

Where, θ_A and θ_B are the advancing and receding contact angle for drainage and imbibition, respectively. Since this empirical relationship is dependent on the radius it can be in cooperated in the Washburn equation, replacing the variables: surface tension and contact

Surface type	*Contact angle*	*Advancing*	*Receding*	*Comments*	*Reference*
Sandstone	140°				Matthews et al, 1995
Sandstone (Roughness)	180°				Matthews et al, 1995; Good,1981
Clay minerals	139°-147°				Diamond, 1970
Kaolin clay		162°	158°		Romero and Simms, 2008
Bituminous coals	130° +- 3°				Spitzer, 1981
brown coals / Lignites	135° +- 3°				Spitzer, 1981
Fused silica		135°-138°	119.5°-121°	For 20%-100% humidity	Good, 1981
Fused silica (outgassed@750°)		105°	90°-95°		Good, 1981
Cement paste	170°-175°				Good, 1981
Anodic Aluminium Oxide membrane		140°-143°	101.7 °-140°		Salmas and Androutsopolous, 2001
Pore glasses		143°	100.5°-107.5°		Salmas and Androutsopolous, 2001
Nuclepore materials		143°	118°-121°		Salmas and Androutsopolous, 2001
Tungsten		130°-142°	132°-121°	at 25°	Ellison *et al.*, 1967
Stainless steel		133°-146°	132°-124°	at 25°	Ellison *et al.*, 1967
Nickel		139°-148°	123°-138°	at 25°	Ellison *et al.*, 1967
Quartz		132°-147°	115°-134°	at 25°	Ellison *et al.*, 1967
Glass		133°-147°	122°-134°	at 25°	Ellison *et al.*, 1967
Teflon		134°-157°	104°-132°	at 25°	Ellison *et al.*, 1967
Soil	130°				Lamotte 1997

Table E1: Contact angles obtained for mercury-air system on different solids, used in the MIP literature.

Appendix E: Mercury saturation, as a result of vapour transport

According to: Transport of elemental mercury in the unsaturated zone from a waste disposal site in an arid region, Walvoord et al., 2008

A research conducted by Walvoord *et al.*, 2008, focusses on the transport of elemental mercury through the unsaturated zone. It concerns a filled burial landsite, in which mercury vapor is leached into the groundwater. The article is based upon field data from soil samples and a modelling exercise on horizontal Hg^0-vapor migration through the unsaturated zone. In figure three of this article, Hg^0 depth profiles are given, with figure a and b concerning Hg^0 vapor and figure 3c the total Hg^0 content. From this latter one, the elemental mercury saturation can be determined by using equation E1 and E2. However, first a correction for the presence of Hg^0 vapor is done, by assuming equilibrium between liquid and vapour phase mercury. The parameters used for these calculations are given in table E1, and the equations used for this correction are based up on the ideal gas law and volume, mass and density relationships.

$$C_{Hg(g)} = \frac{n}{V} = \frac{P_{Hg}}{RT} M_{molar} \qquad \text{(eq. E1)}$$

$C_{Hg(g)}$ is the concentration of elemental mercury in the gas-phase [kg m^{-3}], n is the amount of molecules [mol], V is volume of air [m^3], R is the gas constant [J $K^{-1}mol^{-1}$], M_{molar} is the molar density [g mol^{-1}] and T is the temperature [K]. To transfer this into the soil vapour content, it is assumed that the sample is made of water and soil, therefore neglecting any volumetric Hg^0 content. This seems reasonable since the concentration of Hg^0 in the sample ranges between 25-125 µg kg^{-1}. So the soil vapour content at equilibrium is given by:

$$C_{Hg(g)}^{soil} = C_{Hg(g)} \frac{\phi\rho_w + (1-\phi)\rho_{Sediment}}{\rho_{Hg}} \qquad \text{(eq. E2)}$$

The results of this correction are visualized by figure F1, it appears that the correction is not significant. Next the liquid mercury saturation (S_{Hg}) is estimated by using equation E3 and E4, both equations are based upon the mass, volume and density relation for each phase. These coupled equations are solved by iterating; initially the S_{Hg} is put to 0.05, and by using equation E3 the density of the sample is calculated, which then is used in equation E4. It is assumed that the porous media is saturated with water to get a maximum S_{Hg} for the system, even though the measurements were done on an unsaturated zone.

$$\rho_{sample} = (1-\phi)\rho_{sediment} + \phi S_{Hg}\rho_{Hg} + \phi(1-S_{Hg})\rho_w \quad \left[\frac{kg}{m^3}\right] \qquad \text{(eq. E3)}$$

$$S_{Hg} = C_{Hg} \frac{\rho_{sample}}{\phi\ \rho_{Hg}} \quad \left[\frac{m_{Hg}^3}{m_{sample}^3}\right] \quad \text{(eq. E4)}$$

This article mentions transport via vapour phase as source of mercury content in the vicinity of a burial site. Therefore saturations obtained are thought to be representative for condensation of mercury vapour rather than liquid mercury flow (i.e. saturations in the order of 10^{-7} to 10^{-8}).

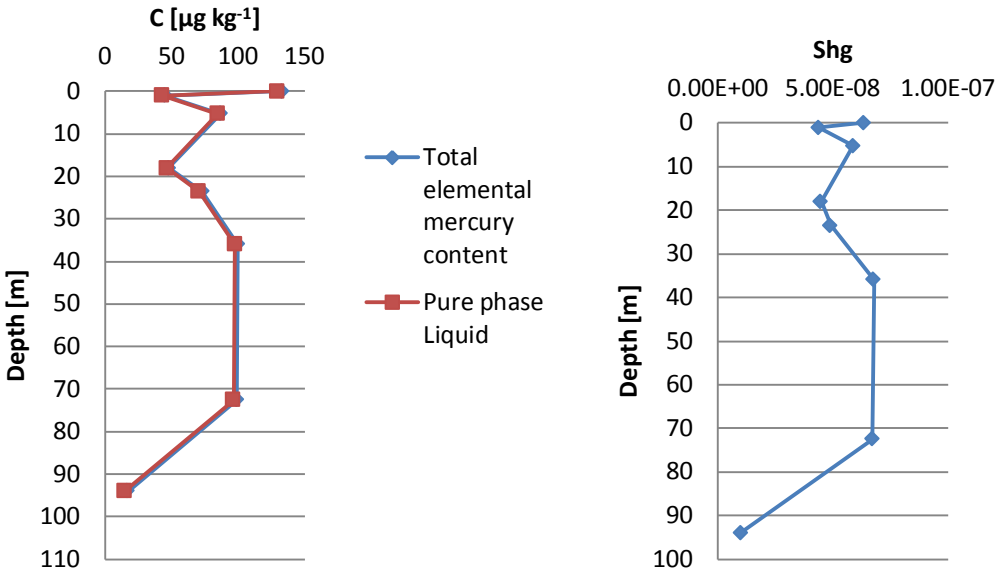

Fig. E1, Hg^0 depth profiles for case study on landfill burial site in Nevada (Walvoord et al., 2008). A) Total and pure phase liquid Hg^0 content in soil. B) Estimation of liquid mercury saturation

Physical property		*Units*
Vapor Pressure	0,18	Pa
Bulk Density	2650	kg m^{-3}
Gas Constant	8,314	J K^{-1} mol^{-1}
Temperature	298,15	Kelvin
Molar mass	200,15	g mol^{-1}

Table E1: Physical properties used for calculations during this appendix. Vapor pressure is according to Wang et al., 2012, other data are typical values. Other soil properties are according to Walvoord et al., 2008.

Appendix F: In-situ DNAPL saturation: Image processing software

Data on DNAPL characteristics in natural soils are uncommon, since in-situ soil samples are not easily accessible. In order to obtain an idea of these characteristics a probing technic was used to make photos at depth within a natural soil. In this manner, a soil depth profile is visualized and can be used to estimate the amount of DNAPL present. Along with this is the data on friction and water pressure during drilling, which is used to determine the different types of soil over depth.

F.1 Mercury volumetric content determination in R

Percentage of mercury in a photo serves as a proxy for the volumetric mercury content. Image processing software can determine the amount of mercury present by interpreting the presence of mercury for each pixel. Software used, is the open source software R, statistical based software in which packages can be included. For image processing the package EBimage is used (www.bioconductor.com (11-02-2013); Pau *et al*., 2010). Two methods were applied on estimating the mercury content, each focusses on a slightly different mercury blob size and therefore all slightly under estimate volumetric mercury content. However, this method is applied solely for estimating mercury content and not for precise parameterisation. Two methods are based on filtering by using two thresholds in a grey-scaled matrix of the photo, whereas the third method uses a drawing method (opening and closing) in a coloured matrix and a single threshold in a grey-scaled matrix.

Thresholding: Filtering of certain colours can be done by using a threshold, since colour is represented as a real number. If a value exceeds the threshold it is given an integer 1 or 0, with 1 being mercury and 0 being anything else. This results in a matrix with 1's and 0', indicating presence of elemental mercury.

Opening and closing: This method is a procedure to connect disconnected areas of multiple pixels with a similar colour (Pau *et al.,* 2012). This method is applied before thresholding, such that larger mercury blobs can be accounted for.

First, to remove background noise (i.e. soil colour interfering with the colour of mercury), a 2D-Gaussian blur method is applied (Pau *et al*., 2010). After producing a 'blurred' photo containing the back ground noise (Fig. F1-B), it is subtracted from the original photo resulting in a smoothed photo (Fig. F1-C). This is used for further analyse, by either using opening or closing or colour filtering.

Filtering of colour is based on applying a threshold and allocates a number 1 or 0 to each pixel. In the end, applying a filter without opening and closing yields a poor result, hence is not suitable for determining an approximation of mercury content (fig. F1-D, F1-E). When using opening and closing method along with a single filter, the result obtained seems reasonable (fig. F1-F and F1-G). Therefore opening and closing method is used with a opening radius of 16 and a closing radius of 6 within a spherical shape.

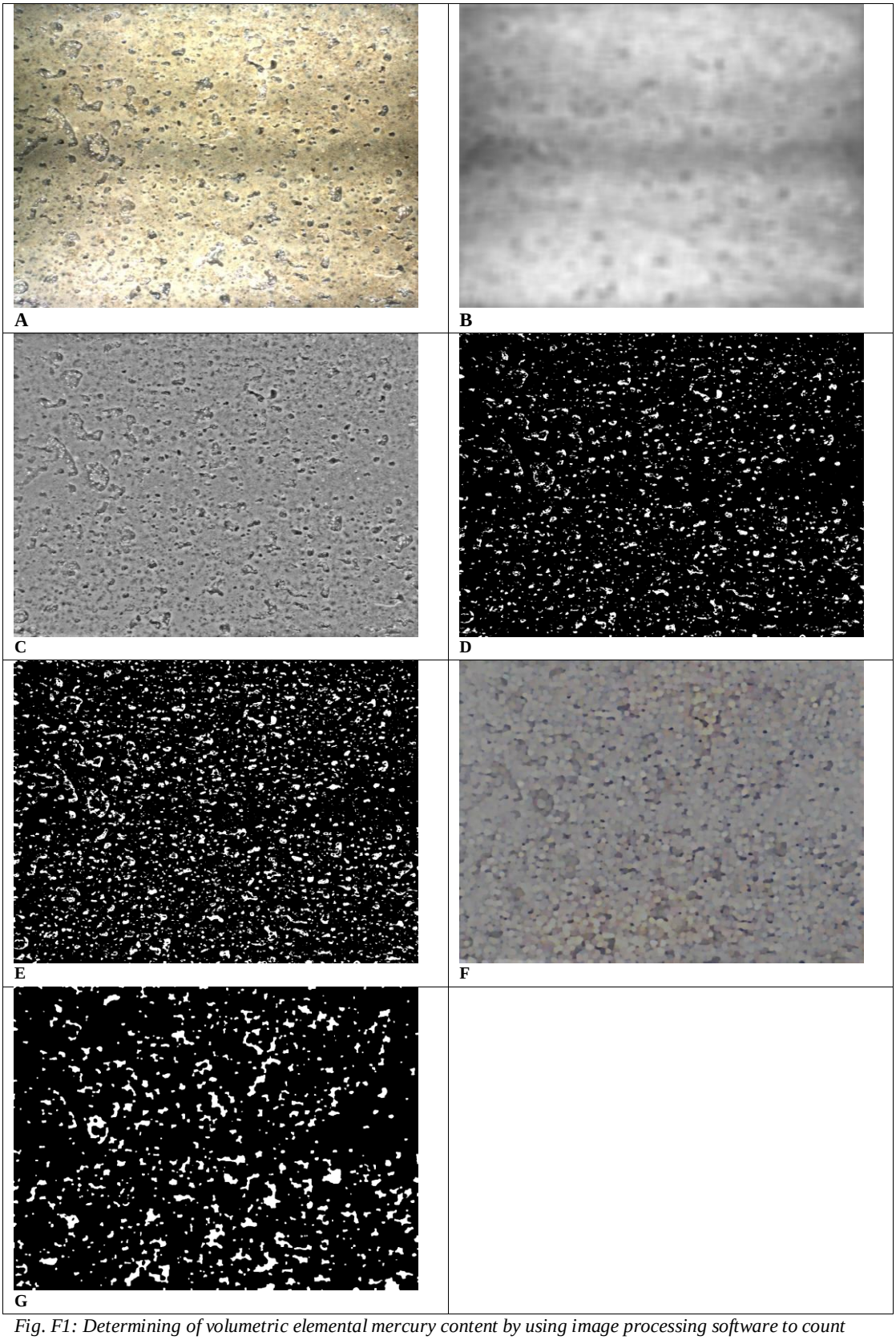

Fig. F1: Determining of volumetric elemental mercury content by using image processing software to count pixels, representing mercury. Size of the photo is 1200 by 1600 pixels or 12 by 18 mm. A) Original photo. B) Blurred photo, by using a Gaussian filter to correct for the background noise. C) Normalized photo, in grey-scale. D) Minimum amount of filtered volumetric mercury content, white indicates the presence of mercury. E) Maximum amount of filtered volumetric mercury content, white indicated the presence of mercury. F) Applied opening and closing method to connect disconnected pixels. G) Volumetric mercury content by using opening and closing method, white indicates the presence of mercury